STRENGTH AND DILATANCY OF CRUSHABLE SOILS WITH DIFFERENT GRADINGS

ZONG-LEI DONG[1], CHEN-XI TONG[2*], SHENG ZHANG[3], YI PIK CHENG[4], DAICHAO SHENG[5]

1. Ph. D candidate, School of Civil Engineering, Central South University, Changsha, 410075, China. Visiting student, School of Civil, Environmental and Geomatic Engineering, University College London, London, WC1E 6BT, England.

Email: dongzl@csu.edu.cn

2. Associate Professor, School of Civil Engineering, Central South University, Changsha, 410075, China.

Email: cxtong@csu.edu.cn (corresponding author)

3. Professor, School of Civil Engineering, Central South University, Changsha, 410075, China.

Email: zhang-sheng@csu.edu.cn

4. Associate Professor, School of Civil, Environmental and Geomatic Engineering, University College London, London, WC1E 6BT, England.

Email: yi.cheng@ucl.ac.uk

5. Distinguished Professor, School of Civil and Environmental Engineering, University of Technology Sydney, Ultimo, NSW 2007, Australia.

Email: daichao.sheng@uts.edu.au

ABSTRACT: Peak strength and dilatancy of granular materials generally decrease with increasing mean effective stress, and such a decrease will be enhanced due to the occurrence of particle breakage. This paper presents a simple empirical approach to modify Bolton's original strength and dilatancy equation for crushable soils with different crushability. The proposed approach is based on data of a series of drained triaxial tests on carbonate soils with five different particle size distributions (PSDs) and three initial relative densities. It is also validated against other published experimental data on various crushable soils, including carbonate soils, limestones, coarse aggregates, and silica sands. The modified relation retains a similar form to Bolton's equation with only one additional parameter introduced. As a result, the crushing strength-related parameter in the original relation is modified to incorporate the impacts of particle shape, gradings, and mineralogy on particle breakage. This modified parameter tends to increase as soil crushability decreases, which keeps a similar physical meaning to Bolton's crushing strength-related parameter, and is suitable for a wider range of crushable soils with different gradings. The proposed strength and dilatancy equation for crushable soils yields to Bolton's equation for strong soil particles where particle breakage is negligible.

Keywords: strength; dilatancy; granular material; particle breakage; crushability

1. Introduction

Granular soils experience interparticle sliding, rolling, and interlocking under shear stress, leading to volume changes either in contraction or dilation. It is widely accepted that the shear strength of granular soils comprises two components: critical state strength and additional strength induced by dilatancy (Bolton, 1986; Chakraborty and Salgado, 2010; Arda and Cinicioglu, 2021). The strength-dilatancy relation, linking soil's strength and deformation, is important for predicting soil strength in engineering construction. Previous studies have developed approaches to determine the bearing capacity of shallow foundations by incorporating the strength-dilatancy relation, considering nonlinear soil strength and progressive failure (Perkins and Madson, 2000; Lau and Bolton, 2011a, 2011b). Using Bolton's strength-dilatancy equation (Bolton, 1986), Jamiolkowski et al. (2003) evaluated the peak friction angle based on data of cone penetration tests and flat dilatometer tests. Recently, the expanding civil engineering industry in China has faced challenges in large projects like island and reef engineering, giant dam constructions, and high-fill airport projects. In these projects, granular soils, which serve as the primary fill material and bear substantial upper loads, inevitably experience significant particle breakage. For example, carbonate soils, known as bioclastic deposits, are susceptible to crushing at low or medium stress levels and are commonly classified as 'problematic soil'. Taking pile foundation engineering on carbonate soil as an example, the pile penetration causes damage to the soil structure at the pile sides, which decreases the dilation and reduces the lateral resistance. This breakage-induced impairment of strength and dilatancy is the main reason for the low bearing capacity of carbonate soil foundations (Yasufuku, 1995). Therefore, an in-depth investigation to the strength-dilatancy relation of crushable soils is of practical engineering importance in addressing these challenges.

Based on the minimum energy ratio principle, Rowe (1962) proposed a widely used stress-dilatancy relation that incorporates soil strength and dilatancy rate. However, it assumes that the strength and dilatancy of an assembly depend on interparticle friction by neglecting the effect of particle breakage, and generally overestimates the dilatancy of granular materials (Wan and Guo, 1998). Such overestimation is supported by subsequent laboratory observations that particle breakage leads to a reduction in strength and impairment of dilatancy of sands (McDowell and Bolton, 1998; Coop et al., 2004). Hence, more attention has been paid to the effect of particle breakage on the strength and dilatancy behaviour of granular soils (Cheng et al., 2003 & 2004; Phuong et al., 2018). Some studies have modified Rowe's theory by introducing energy consumption due to particle breakage E_b (Ueng and Chen, 2000; Salim and

Indraratna, 2004; Tarantino and Hyde, 2005). However, breakage energy is difficult or even impossible to measure directly. It is commonly back-calculated by subtracting friction energy and dilatancy energy from the total energy input. Guo and Zhu (2017) found that if one follows the assumption that the friction coefficient M equals the critical state stress ratio M_c when calculating the friction energy, the calculated E_b may be negative at the onset of shear and decrease with increasing strain especially when dilation occurs. Although some attempts have been made to address this problem, those approaches are still complex in form and involve many fitting parameters without clear physical meaning.

On the other hand, Bolton (1986) aimed to develop a strength and dilatancy relation that is simple in form and easy to apply in engineering practice. Based on experimental data of 17 silica sands in triaxial shear and plane strain conditions, Bolton (1986) proposed the famous empirical strength-dilatancy relation, which has been widely used in theory and engineering practice (Lau and Bolton, 2011a; Jamiolkowski et al., 2003). Bolton's equation is expressed as

$$\varphi'_{\mathrm{p}} - \varphi'_{\mathrm{cs}} = b\psi_{max} = mI_{\mathrm{R}} \tag{1a}$$

$$I_{\mathrm{R}} = D_{\mathrm{r}}(Q - \ln\, p'_{\mathrm{f}}) - R \tag{1b}$$

where the difference in effective friction angle (φ'_p-φ'_{cs}) represents the shear strength contributed from dilatancy with φ'_p and φ'_{cs} being the effective friction angle at peak and critical state, respectively. The maximum dilatancy angle, ψ_{max}, is commonly assumed to be equal to the peak dilatancy angle ψ_p (Bolton, 1986). The value of b is 0.8 for plane strain and 0.48 for the triaxial condition, as implied by Bolton (Bolton, 1986; Chakraborty and Salgado, 2010). I_R is the relative dilatancy index, it is valid for $0 \leq I_R \leq 4$ and is set to be 4 when $I_R > 4$, p'_f is the mean effective stress at failure, D_r is the initial relative density. The value of m is set to be 3 for triaxial shear and 5 for plane strain. Q and R are dimensionless empirical parameters, with R = 1. According to Bolton (1986), the collected silica sands data satisfies Q = 10. As indicated in Equation (1), only parameter Q is unknown, therefore, in theory, only one reliable triaxial test is needed to determine Bolton's equation. Engineers can then predict the soil's strength under other soil states.

Bolton's relation has been widely used and modified to accommodate additional factors such as fine or gravel content, initial grading, test type, stress path, stress level, and particle breakage. For example, Simoni and Houlsby (2006), and Xiao et al. (2014) modified Bolton's relation to take into account the influence of gravel content and fine content on mixed soils, respectively. Chakraborty and Salgado (2010) and Amirpour Harehdasht et al. (2017; 2019) made their modifications in terms of stress level, type of test, initial PSD, etc. The details are summarized in Table 1. Among these, some modified equations introduced more than two extra parameters without clear physical meaning, while some are not applicable to the triaxial stress path and are different in form from Bolton's equation.

Table 1 Modification of Bolton's original strength-dilatancy relation in the literature

Author(s)	Proposed relation	Notes
Jamiolkowski et al., 2003	$\varphi'_{\mathrm{p}} - \varphi'_{\mu} = mD_{\mathrm{r}}\ln(\sigma'_{\mathrm{c}}/p'_{\mathrm{f}}) \quad \varphi'_{\mathrm{p}} \geq \varphi'_{\mu} + m$ $\varphi'_{\mathrm{cs}} - \varphi'_{\mu} = 3°$ for triaxial shear $\varphi'_{\mathrm{cs}} - \varphi'_{\mu} = 5°$ for plane strain	φ'_{μ} is the pure friction angle defined by Rowe (1962), σ'_{c} is a threshold stress in 1-D compression test.
Simoni and Houlsby, 2006	$\varphi'_{\mathrm{p}} - \varphi'_{\mathrm{cs}} = 5I_{\mathrm{R,\,mix}}$ $I_{\mathrm{R,\,mix}} = 5D_{\mathrm{r,\,mix}} - (1 - 4.3 \cdot \Delta e)$ $\Delta e = e_{\mathrm{min,sand}} - e_{\mathrm{min,mix}}$	Modification for sand-gravel mixtures in direct shear tests. $D_{\mathrm{r,mix}}$ is relative density of the mixture, $e_{\mathrm{min,sand}}$, $e_{\mathrm{min,mix}}$ are the minimum void ratios of host sand and the mixture.
Hamidi et al., 2009	$\varphi'_{\mathrm{p}} - \varphi'_{\mathrm{cs}} = 5D_{\mathrm{r,\,mix}} - [1 + (4.5 - 0.006\sigma_{\mathrm{v}}) \cdot \Delta e]$ $\Delta e = e_{\mathrm{min,sand}} - e_{\mathrm{min,mix}}$	Modification for sand-gravel mixtures in direct shear tests considering particle breakage, where σ_{v} is the normal pressure.
Chakraborty and Salgado, 2010	$\varphi'_{\mathrm{p}} - \varphi'_{\mathrm{cs}} = 3.8I_{\mathrm{R}} = 3.8[D_{\mathrm{r}}(Q - \ln\, p'_{\mathrm{f}}) - R]$ $Q = 7.4 + 0.60\ln\, \sigma_{\mathrm{c}}$ for triaxial shear $Q = 7.1 + 0.75\ln\, \sigma_{\mathrm{c}}$ for plane strain	Modification for low confining pressures (< 196 kPa) in triaxial shear and plane strain.
Xiao et al., 2014	$\varphi'_{\mathrm{p}} - \varphi'_{\mathrm{cs}} = \alpha_{\varphi}[D_{\mathrm{r}}(Q - \ln\, p'_{\mathrm{f}}) - R]$ $\alpha_{\varphi} = \alpha_{\varphi 0} + \chi_{\alpha}\exp\,[-\exp\,(-F) - F + 1]$ $F = (f_{\mathrm{c}} - f_{\mathrm{co0}})/k_{\mathrm{f}}$ $Q = Q_0 + \chi_Q \ln\left(100(\sigma_{\mathrm{c}} - \sigma_Q)/p_{\mathrm{A}}\right), R = 1$	Modification for silty sands. f_{c} is fine content; f_{c0}, k_{f}, χ_{α}, Q_0, χ_Q, σ'_Q are the material parameters. $\alpha_{\varphi 0}$ is the α_{φ} when $f_{\mathrm{c}} = 0$.
Amirpour Harehdasht et al., 2017; 2019	$\varphi'_{\mathrm{p}} - \varphi'_{\mathrm{cs}} = b\psi_{max}$ $\varphi'_{\mathrm{p}} - \varphi'_{\mathrm{cs}} = mI_{\mathrm{R}} = m[D_{\mathrm{r}}(Q - \ln\, p'_{\mathrm{f}}) - R]$ $b = c_1(d_{50})^{-c_2}, m = c_3(d_{50})^{-c_4}$	Modification for considering the effect of initial PSD in plane strain and triaxial shear, where d_{50} is the mean particle size, c_1-c_4 are the fitting parameters.

It is worth noting that most sands used in Bolton's research are silica-based sands with strong grains and are considered less crushable within the stress range tested, as compared to crushable carbonate soils. For fragile materials, Bolton (1986) suggested smaller values of Q based on Billam's experimental data (Billam, 1972). This suggestion was supported by Jamiolkowski et al. (2003) (observing $Q = 9.5$ for Kenya sand and 7.5 for Quiou sand) and Airey et al. (1988) ($Q = 8.8$ for Halibut sand and 7.9 for Kingfish sand). For uniformly graded soils, Bolton (1986) considered that the value of the parameter Q is related to the crushing strength of soil grains, and therefore linked the parameter Q to the characteristic stress σ_0 that can represent the crushing strength of grains (McDowell and Bolton, 1998), which is expressed in Equation (2).

$$I_R = D_r \ln\left(\frac{A\sigma_0}{p'_f}\right) - 1 \tag{2}$$

where A is a scalar multiplier. In fact, the crushability of soils with different gradations is more complex. Correlating the value of Q purely to particle crushing strength is not sufficient. For crushable soils with different initial PSDs, particle breakage impairs the degree of dilatancy, causing a more pronounced decrease in φ'_p-φ'_{cs} with increasing p'_f, which was supported by laboratory testing data (Datta et al., 1979; Ueng and Chen, 2000; Kuwajima et al., 2009; Nicks and Adams, 2018). Figure 1(a) depicts carbonate sands tested by Datta et al. (1979) with two different gradations having similar uniformity coefficients C_u (1.46 and 1.53) but different mean particle sizes d_{50} (0.97 mm and 0.24 mm). The carbonate sand with d_{50}=0.97 mm is more crushable, showing a larger reduction rate in φ'_p-φ'_{cs} with lnp'_f. Nicks and Adams (2018) also observed that the poorly graded coarse aggregate with d_{50} = 17.02 mm has a faster reduction rate of φ'_p-φ'_{cs} with lnp'_f than that with d_{50} = 8.64 mm, as shown in Figure 1(b). It can be seen that Bolton's relation underestimates the shear strength of crushable granular soils at low stresses and overestimates it at high stresses, such as carbonate sand with d_{50}=0.97 mm and coarse aggregate with d_{50}=17.02 mm. For the less crushable soils, Bolton's relation performs better. This is because Bolton's Equation (1) has a limitation where the reduction rate is identical for all sands at a given relative density D_r, which is not appropriate for some crushable materials. The more crushable the material, the less accurate Bolton's relation becomes, indicating the necessity for modification.

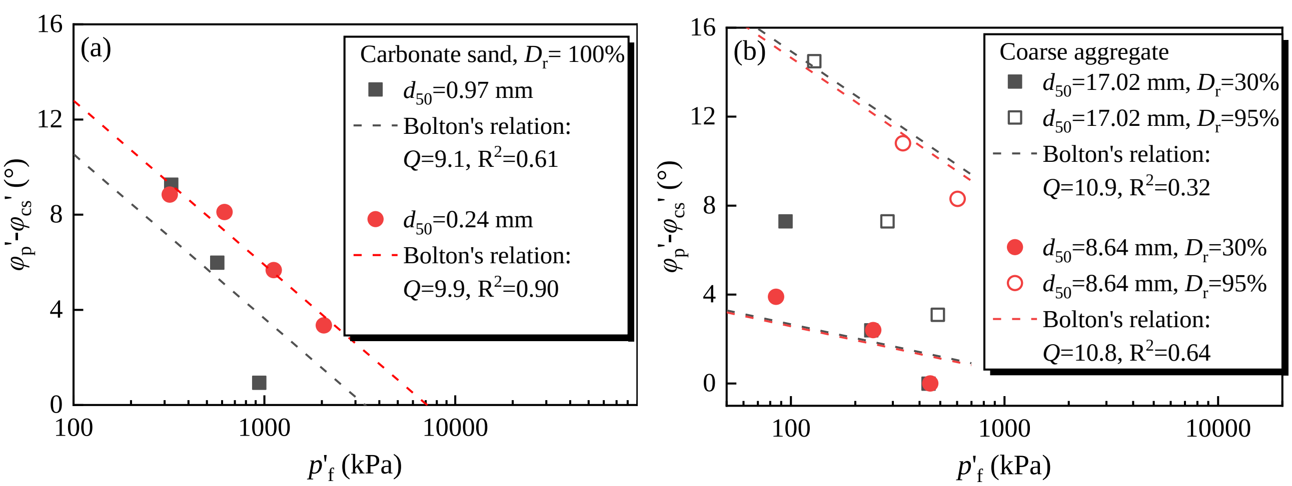

Figure. 1. The limitation of Bolton's relation illustrated using (a) carbonate sand data from Datta et al. (1979) and (b) coarse aggregates data from Nicks and Adams (2018)

For this purpose, this paper attempts to propose a modification in this paper by introducing one additional parameter B. This additional parameter is related to the wider effects of particle angularity and gradings together causing a different decreasing rate of strength and dilatancy of crushable soils. The modification is then validated against the results from a series of drained triaxial tests on carbonate soils and other published experimental data on crushable soils, and the physical meaning of parameters of the modified relation is further explored. The proposed empirical relation shows the advantage of simplicity in relating the crushability of granular soils to their mechanical behaviour, and is useful for engineers to estimate the strength of crushable soils.

2. The modified strength and dilatancy relation

2.1 The purpose of the modified relation

For crushable soils, when an assembly is under deviatoric stress, the interlocked grains will crush. The broken pieces fall into the void space, the sample repacks itself in a denser arrangement, leading to enhanced compressibility, and impairment of dilatancy (McDowell and Bolton, 1998). Consider two identical samples with angular particles, one more crushable (represented in red) and the other almost non-crushable (represented in black), as shown in Figure 2. At low stresses, where particle breakage is negligible, the dilatancy of the crushable and the non-crushable samples should be similarly high. However, the crushable sample exhibits less dilation at high stresses compared to the non-crushable sample. In other words, within the same stress range, the dilatancy of the crushable soil has a larger variation. The initially very high dilatancy at low stress was suppressed at a much faster rate than normal as stress increased. This stress-related suppression rate is related to the level of particle breakage, which varies at high stresses according to an average coordination number of an assembly depending on gradings, resulting in a different decreasing rate of strength and dilatancy. As shown in Equation (1b), the relative dilatancy index I_R is controlled by the initial relative density and stress. The limitation of Bolton's equation in capturing a faster reduction of φ'_p-φ'_{cs} with lnp'_f can be attributed to the limitation of using the initial relative density D_r. When the soil is more crushable, the initial PSD was altered more significantly by the crushing of particles, making it necessary to modify D_r to improve accuracy.

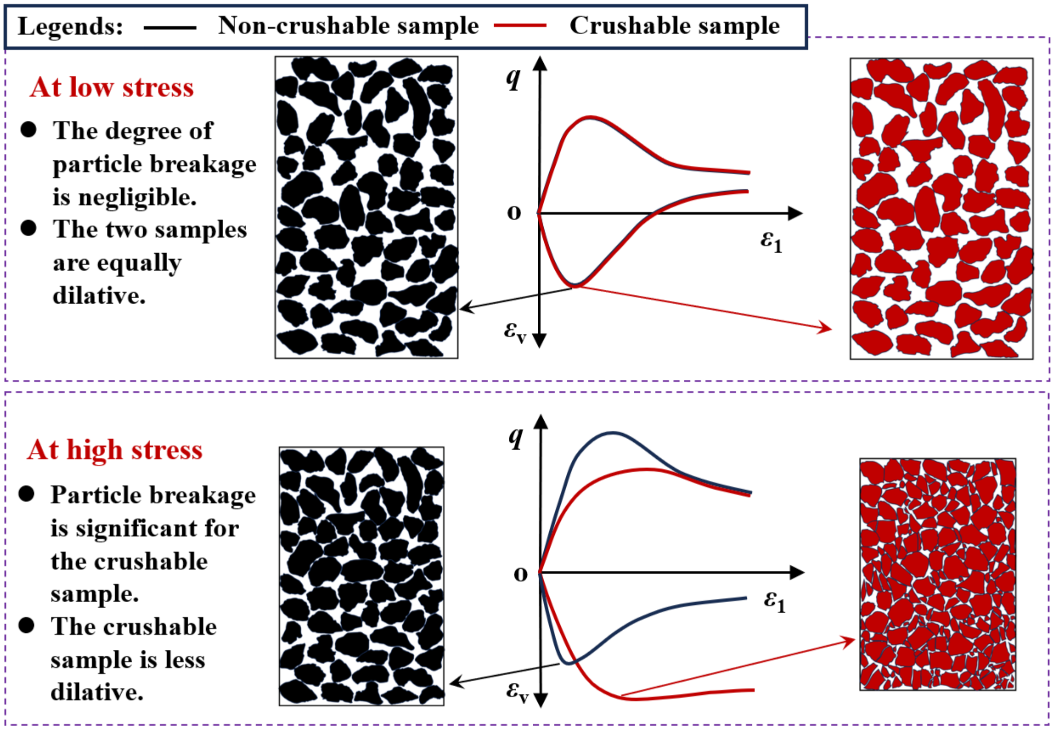

Figure 2. The Schematic diagram of dilatancy impairment due to particle breakage

To account for the change in soil structure resulting from particle breakage, we introduce an additional empirical parameter *B*, which modifies the initial relative density to a suitable value as particle breakage occurs. The parameter *B* can also be used as a rate-related factor to allow for a different rate of change of φ'_p-φ'_{cs} with lnp'_f. The modified relation is then expressed as

$$\varphi'_{\mathrm{p}} - \varphi'_{\mathrm{cs}} = b\psi_{max} = mI_{\mathrm{R}}^{*} \tag{3a}$$

$$I_{\mathrm{R}}^{*} = D_{\mathrm{r}}B\left(Q^{*} - \ln\frac{p'_{\mathrm{f}}}{p_{\mathrm{r}}}\right) - R \tag{3b}$$

where I_R^* is the modified relative dilatancy index; p_r is a reference pressure (= 1 kPa) for ensuring dimensional consistency. m = 3 for triaxial tests and R = 1 as suggested by Bolton (1986). *B* is a rate-related parameter, $Q^* = Q/B$ because of the introduction of parameter *B*.

Figure 3 shows the schematic diagram of the original and modified relation. The original and modified relations are similar in form, differing only in the slope of the lines. In both cases, φ'_p-φ'_{cs} increases with increasing initial relative density D_r and decreases with increasing mean effective stress at failure p'_f. Both the original and modified relations represent sets of straight lines in the (φ'_p-φ'_{cs})-lnp'_f plane converging at a point with coordinates (p_c, -mR). This imaginary convergent stress p_c is important because it expresses some intrinsic features of the material. For a given material with a specific initial PSD, the convergent stress p_c is unique regardless of the soil states (e.g., the initial relative density and the stress level (Been and Jefferies, 1985)). Specifically, the natural logarithm of p_c is equivalent to Q in the original relation and Q^* in the modified relation. Bolton (1986) suggested that the value of Q is related to the soil crushability, implying that p_c might be a stress associated with particle crushing. The Q^* of the modified relation has the same expression as Bolton's equation (= ln p_c), indicating that the Q^* may be a substitute for Q, which is also related to soil crushability. The detailed evidence will be given later.

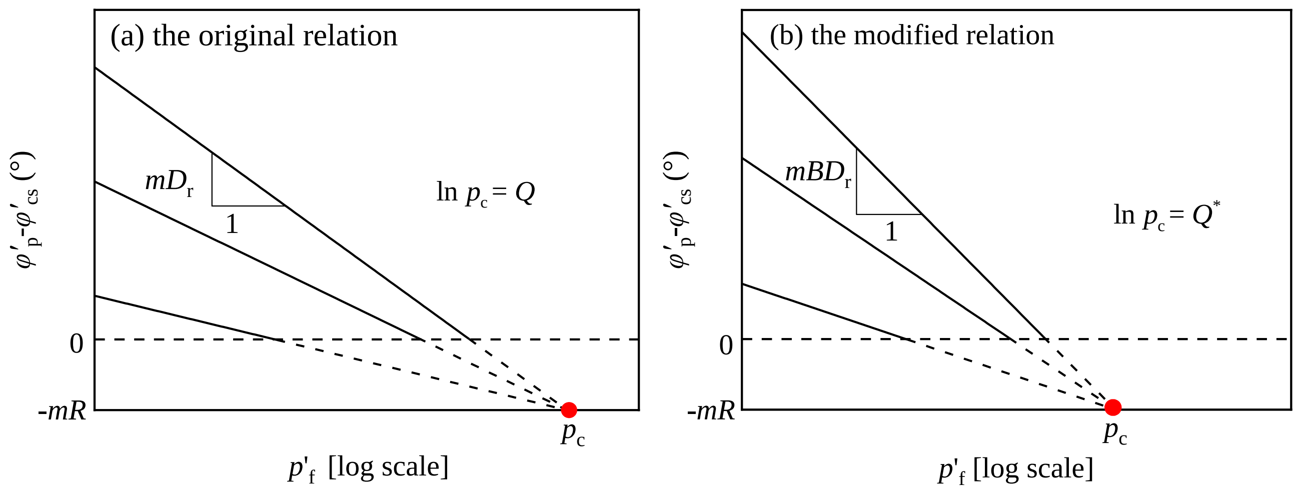

Figure 3 Schematic diagram of (a) the original and (b) the modified strength-dilatancy relation

2.2 Methodology

The validation process of the modified relation was twofold: through experimental validation as designed in this paper, and by using data available in published literature. These components were elaborated in Section 3 and Section 4, respectively. The correlation between the parameters of the modified relation and soil crushability was investigated and is presented in Section 3.4.

For model validation using experimental data, a series of drained triaxial tests were conducted on carbonate soils with different initial PSDs. In general, a uniform-graded sample will suffer more particle breakage, and hence be more crushable than a well-graded one for a given stress path. Five initial PSDs, representing different crushability, were adopted in this paper. The modified relation was then validated using these experimental data.

Published data in the literature were adopted to further validate the modified relation. Four types of materials were mainly employed. The first type is carbonate soils used as foundation fills for offshore engineering, which are widely recognised as crushable soils. The second type is coarse aggregates such as rockfills used in constructing retaining walls, pavement bases, and dams. They commonly have larger particle sizes and are susceptible to crushing since the crushing strength of particles typically decreases with increasing particle size (McDowell and Bolton, 1998). The third type includes limestone, anthracite, and chalk, crushable materials mentioned in Bolton's (1986) paper. Using the same dataset for comparison, we found that the modified relation provided a better fit. The fourth type is silica sands, used to demonstrate that the modified relation can degrade to Bolton's equation for less crushable silica sands.

The proposed modified relation (i.e., Equation (3)) can be rewritten in the following linear form.

$$\frac{(\varphi'_{\mathrm{p}}-\varphi'_{\mathrm{cs}})/m+R}{D_{\mathrm{r}}} = Q^{*}B - B\ln\ p'_{\mathrm{f}} \tag{4}$$

where $m = 3$ and $R = 1$ as Bolton suggested (Bolton, 1986). Letting $Y= [(\varphi'_{\mathrm{p}}-\varphi'_{\mathrm{cs}})/m+R]/D_{\mathrm{r}}$ and $X= \ln p'_{\mathrm{f}}$, the values of parameters Q^* and B can be obtained using simple linear regression. It can be seen that only two parameters, Q^* and B, are unknown in the modified relation. After determining these two parameters of the modified relation using equation (4), we can predict the soil's strength under different states (e.g., different initial relative density and different stress level (Been and Jefferies, 1985)).

In this paper, the modified strength and dilatancy relation remains consistent with Bolton's equation in terms of assumptions. The peak strength of granular soil consists of two components, the critical state strength and the strength contributed by dilatancy. The critical state strength is constant for a specific material. It is also assumed that no particle breakage occurred during the initial consolidation process, so only the shearing data of normally consolidated soils is used in the validation process. Dilative behaviour is controlled by the soil's state relative to the critical state line on the volume-stress plane before shearing. For soils initially loaded to a very high-stress level, resulting in significant particle breakage, the grading changes. In such cases, further research on the parameters in the modified relation is required. Additionally, the materials selected for validation do not include binary mixtures, such as sand-silt mixtures or sand-gravel mixtures. Further investigation is needed to assess the applicability of the modified relation for these materials.

3. Model validation using test data

3.1 Tested materials and method

The materials tested in this study are hydraulic-filled carbonate soils found on a coral reef island in the South China Sea. These soils have a high $CaCO_3$ content of 96.88% and are characterized by well-developed internal pores, irregular shape, low strength, and high brittleness. The original material was sieved to produce samples with five different PSDs (gradings A-E) based on ASTM standard (ASTM C136/C136M, 2014), as shown in Figure 4.

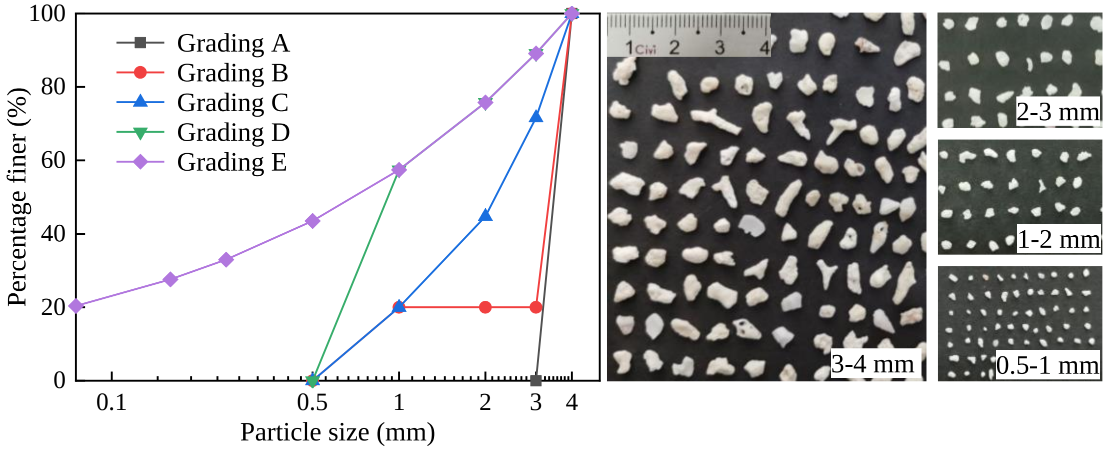

Figure 4 The initial PSDs of the tested carbonate soils

According to the Standard for Geotechnical Testing Method (GB/T 50123-2019), the minimum void ratio e_{min} is measured by hammering the top of a soil sample while applying vibration on both sides. This process can cause particle breakage for crushable soils, altering their initial PSDs. To avoid particle breakage occurring, some researchers only retained the vibration part when measuring e_{min} (Zhang, 2000). This modified approach is adopted in this study, while the test for maximum void ratio e_{max} still follows the method in GB/T 50123-2019, where dry sands with a given mass are slowly poured into a measuring cylinder to reach the loosest state. Table 2 presents the physical properties of the tested carbonate soils.

Table 2. Basic physical parameters of the carbonate soil with different initial PSDs

Initial PSD	G_s	e_{max}	e_{min}	d_{50}	C_u	C_c
Grading A	2.83	1.61	1.11	3.50	1.16	0.98
Grading B	2.83	1.42	0.92	3.34	4.65	3.73
Grading C	2.83	1.37	0.88	2.16	3.43	1.02
Grading D	2.83	1.34	0.86	0.91	1.96	0.84
Grading E	2.83	0.90	0.41	0.69	29.73	0.98

The carbonate soil with grading A is uniform-graded, which is expected to have the greatest particle breakage. Grading B is a discontinuous gradation with the absence of 2-3 mm and 1-2 mm size fractions. Gradings C-D are fractal within 1-4 mm particle size range with the fractal dimension D being 1.84 and 2.6, respectively, while grading E is fractal within particle size of 0.075-4 mm with D = 2.6. The mass of each size fraction of gradings C-E is calculated according to the fractal model proposed by Tyler and

Wheatcraft (1992), which is expressed as:

$$\frac{M(\Delta<d)}{M_{\mathrm{T}}} = \left(\frac{d}{d_{max}}\right)^{3-D} \tag{5}$$

where d and M ($\Delta<d$) are the particle size and the mass of particles smaller than d, respectively; $d_{\max}$ is the maximum particle size; M_{T} is the total mass of particles; D is the fractal dimension.

As shown in Figure 4, grading C has the same small particle content (0.5-1 mm) as grading B (=20%), while grading D has a small particle content of 57.4%. The grading E samples have a fine content (particle diameter d < 0.075mm) of about 20%, which may make their behaviour different from that of the other carbonate soils in this paper (Tong et al., 2022b). It has been widely reported that particle breakage ultimately ceases at a fractal grading. Although the fractal dimension of this ultimate grading remains inconclusive, as it may depend on factors such as the initial PSD and the type of loading, it is commonly reported in the literature to fall within the range of 2.5-2.6 (McDowell and Bolton, 1998; Coop et al., 2004; Fan et al., 2021). Therefore, the grading E samples with a fractal dimension of 2.6 are not expected to crush. As expected, no detectable particle breakage was observed for the grading E samples after shearing. It is not difficult to deduce that the crushability of the A-E graded samples decreases sequentially, which is supported by the post-test sieving results.

A total of 61 sets of drained triaxial compression tests were conducted on the carbonate soils with five initial PSDs at three relative densities and different confining pressures. The initial relative density of a soil sample is controlled by controlling its mass. All samples were prepared with 39.1 mm in diameter and 80 mm in height by the moist tamping method with 0.5% water content to ensure homogeneous distribution of small and large particles (Zhang and Baudet, 2013). Then they were saturated by applying the back pressure of 300-400 kPa with the Skempton's B value greater than 0.95. After saturation, the samples were isotopically consolidated to different confining pressures and then sheared at the strain rate of 0.05%/min until the axial strain reached 25%.

A 1 mm thick rubber membrane was used to avoid puncturing by sharp corners of particles. Appropriate corrections were made to account for the additional volumetric change due to membrane penetration and extra deviator stress caused by rubber membrane, based on the methods proposed by Baldi and Nova (1984) and ASTM standard (ASTM D4767-11, 2020), respectively. The post-test samples were sieved to quantify the degree of particle breakage. According to the sieving results, particle breakage of all samples during sample preparation and consolidation is negligible. Therefore, the particle breakage in our tests all refers to that during the shear stage. Table 3 summarizes the detailed test scheme and results.

In order to ensure the observed dilatancy behaviour, relatively low confining pressures (up to 400k Pa) were adopted for gradings A-D samples. Table 3 records the data at the peak state together with the breakage index B_g (Marsal, 1967) measured at the end of the test. B_g is the sum of the mass difference of each size fraction to the total mass of the sample, defined in detail in Section 3.4. The degree of particle breakage is still evident. A higher amount of particle breakage is observed in dense samples than in loose ones. This trend contrasts with the results typically obtained in one-dimensional compression tests, which is attributed to the effect of the coordination number (Tong et al., 2022b).

Table 3. Summary results of drained triaxial compression tests on the carbonate soils

Initial PSD	Test setup		φ'_{cs} (°)	Data at peak state			Breakage index
	D_r (%)	σ'_3 (kPa)		p'_f (kPa)	φ'_p (°)	ψ_p (°)	B_g (Marsal, 1967)
Grading A	30	50	39.9	127.37	44.34	10.70	0.088
		100		232.59	41.72	6.18	0.128
		150		333.39	40.33	0.51	0.190
		200		424.11	38.83	-0.63	0.223
	60	50		148.32	48.31	15.86	0.091
		100		257.08	44.59	10.66	0.150
		150		363.34	42.91	4.14	0.192
		200		442.17	40.16	0.58	0.250
	90	50		170.00	51.50	24.32	0.094
		100		289.09	47.67	14.78	0.164
		150		396.59	45.36	10.62	0.243
		200		486.70	43.04	4.32	0.259
Grading B	30	50	39.2	117.57	42.04	7.45	0.061
		100		220.42	40.07	3.49	0.080
		150		327.12	39.73	1.82	0.121
		200		419.13	38.44	-0.18	0.147
	60	50		128.85	44.66	12.40	0.056
		100		240.64	42.72	7.99	0.082
		150		346.59	41.52	4.04	0.119
		200		437.69	39.84	0.41	0.154
	90	50		160.60	50.21	21.87	0.075
		100		273.42	46.24	11.02	0.099
		150		387.05	44.69	9.35	0.147
		200		477.69	42.50	3.61	0.176
Grading C	30	50	39.0	114.54	41.26	6.94	0.014
		100		219.73	39.97	3.40	0.034
		150		323.62	39.39	3.18	0.044
		200		427.29	39.07	1.29	0.051
	60	50		131.49	45.21	15.04	0.013

		100		237.21	42.30	9.82	0.030
		150		347.95	41.63	7.18	0.047
		200		453.39	40.94	3.52	0.052
	90	50		161.82	50.39	26.61	0.019
		100		281.97	47.04	18.19	0.033
		150		399.91	45.58	16.13	0.049
		200		503.22	43.99	9.91	0.060
		400		917.20	41.29	0.48	0.097
Grading D	30	100	38.2	214.81	39.25	5.65	0.012
		200		418.33	38.38	2.92	0.029
		250		513.55	37.78	1.48	0.039
		300		620.06	37.98	0.38	0.049
	60	100		242.07	42.89	12.85	0.017
		200		456.01	41.11	7.02	0.037
		300		635.35	39.68	2.67	0.051
		400		857.69	39.19	1.31	0.068
	90	100		270.51	45.96	20.52	0.014
		200		509.32	44.33	12.23	0.037
		300		723.47	42.78	10.16	0.060
		400		930.19	41.71	3.89	0.074
Grading E	60	100	41.1	247.53	43.53	7.08	—
		200		480.08	42.65	3.09	—
		400		944.46	42.16	2.62	—
		800		1852.20	41.58	2.55	—
	75	100		265.23	45.44	9.97	—
		200		512.34	44.49	6.29	—
		400		982.22	43.30	4.73	—
		800		1907.18	42.45	2.97	—
	90	100		284.68	47.29	13.41	—
		200		542.57	46.04	9.27	—
		400		1032.24	44.70	5.73	—
		800		1996.46	43.76	4.54	—

3.2 Test results

The strength and dilatancy of triaxial test are quantified by the friction angle φ' and dilatancy angle ψ, which can be expressed as (Vaid and Sasitharan, 1992)

$$\sin\,\varphi' = \frac{\sigma_1'/\sigma_3'-1}{\sigma_1'/\sigma_3'+1} \tag{6}$$

$$\sin\,\psi = -\frac{\mathrm{d}\varepsilon_\mathrm{v}}{\mathrm{d}\gamma} = \frac{2}{1-3/(\mathrm{d}\varepsilon_\mathrm{v}/\mathrm{d}\varepsilon_1)} \tag{7}$$

where σ'_1 and σ'_3 are the major and minor effective principal stresses; $d\gamma$ is the shear strain increment; $d\varepsilon_\mathrm{v}$ and $d\varepsilon_1$ are the volumetric strain increment and axial strain increment, respectively.

Figure 5 presents the variation of peak friction angle and dilatancy angle for samples with five different gradations. It can be seen that the φ'_p increases with increasing relative density and decreases with increasing confining pressure at different rates for the carbonate soil with different initial PSDs. For each relative density, the grading A samples have the largest decreasing rate of φ'_p, followed by the gradings B-D samples, while the grading E samples have the smallest decreasing rate. The B_g data from Table 3 also show that for each relative density, the amount of particle breakage is highest for grading A samples, followed by gradings B-D samples while Grading E samples have no particle breakage. The evolution of peak dilatancy angle ψ_p is very similar to that of φ'_p, demonstrating the first-order factor of the dilatancy on the peak friction angle of carbonate soils.

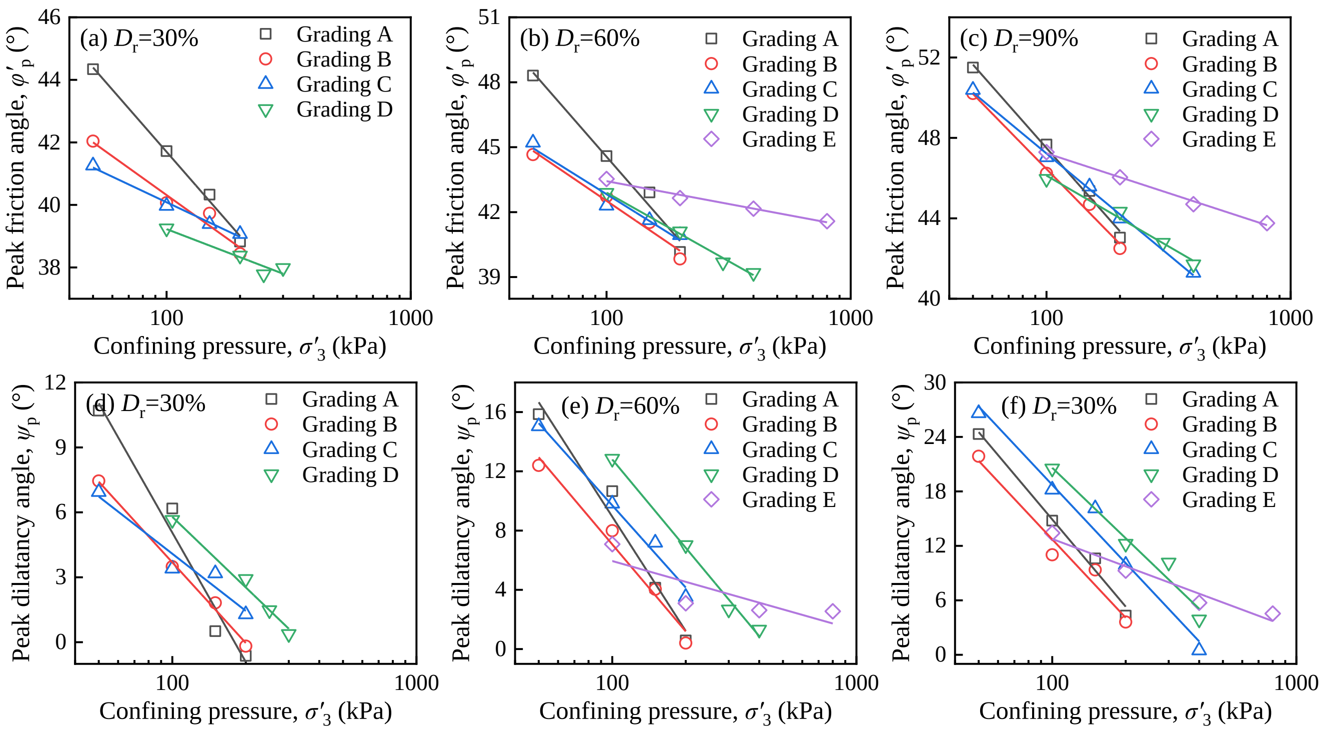

Figure 5 Variation of peak friction angle and dilatancy angle of the carbonate soils with different PSDs

The critical state occurs at constant shear stress and zero volume change when shearing. The critical state friction angle is often derived from experimental extrapolations, based on the fact that critical state holds zero dilation (Bolton, 1986). The relations between peak friction angle φ'_p and peak dilatancy angle ψ_p for the five tested samples (A to E) are presented in Figure 6. The critical state friction angles φ'_{cs} are extrapolated to be 39.9°, 39.2°, 39.0°, 38.2° and 41.1° for the carbonate soil with gradings A-E, respectively. The value of φ'_{cs} sequentially decreases for the carbonate soils with gradings A-D. This may be related to the difference in particle shape (Yang and Luo, 2015).

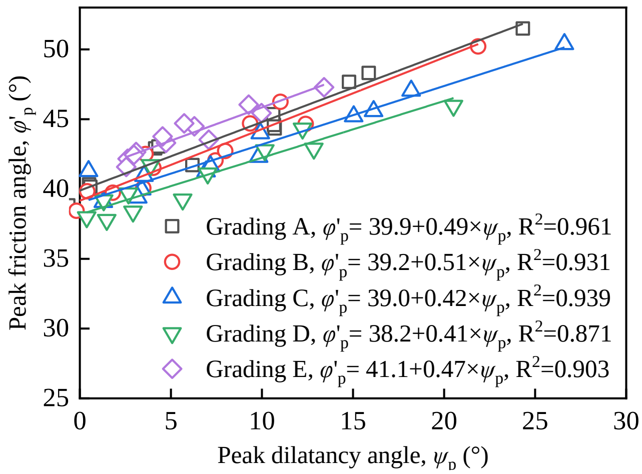

Figure 6 Extrapolation of the critical-state friction angle for the carbonate soils

The particle shape is quantified for carbonate soils with gradings A-D using a photographic and image processing method (Dong et al., 2024). Three 2D particle-shape indices, sphericity, aspect ratio, and convexity, are adopted in this paper based on the work of Altuhafi et al. (2016). The sphericity is calculated as the ratio of the perimeter of the equivalent circle with the same area as the particle to the actual perimeter, the aspect ratio is the ratio between Feret minimum and Feret maximum diameters, and the convexity refers to the ratio of the projected particle area to the convex area. Table 4 shows the particle shape indices for each particle size fraction of gradings A-D.

Table 4 Particle shape indices of different particle size groups

Particle group	Sphericity	Aspect ratio	Convexity
0.5-1 mm	0.880	0.730	0.962
1-2 mm	0.868	0.709	0.956
2-3 mm	0.858	0.701	0.948
3-4 mm	0.835	0.662	0.929

Sphericity, aspect ratio, and convexity gradually decrease as the particle size increases, indicating a more irregular particle shape with increasing particle size. The more irregular particle shape of the larger particle size groups explains why the grading A sample has the highest critical state friction angle. Yang and Luo (2015) created a sequence of mixtures with varying particle shape by mixing spherical glass beads and crushed angular glass beads in different proportions. They found that the value of φ'_{cs} is affected by particle shape but is independent of the initial PSD. Wu et al. (2021) conducted a series of drained shear tests on 12 types of clinker ash with varying particle shapes and proposed a useful mathematical expression to predict the critical state strength, taking into account the effect of particle shape. The conclusion of this paper regarding the influence of particle shape on critical state strength is consistent with the findings of Yang and Luo (2015) and Wu et al. (2021). Figure 6 also shows that the φ'_{cs} of the grading E samples are the highest, which may be attributed to the 20% fine content contained. Further investigation of the effect of fine content on φ'_{cs} is required in the future.

3.3 Model validation

Figure 7 presents the fitting results of the original and modified relations using the experimental data of the carbonate soils. Bolton's equation can also be fitted using Equation (4) where Q^* is replaced by Q and B=1. For a better comparison, both the original and modified relations employed the optimal fit of Equation (4). The superiority of the modified relation over the original relation is obvious. The value of parameter Q^* increases from 6.67 for grading A samples to 10.71 for grading E samples, whereas parameter B decreases from 4.08 for grading A samples to 0.62 for grading E samples.

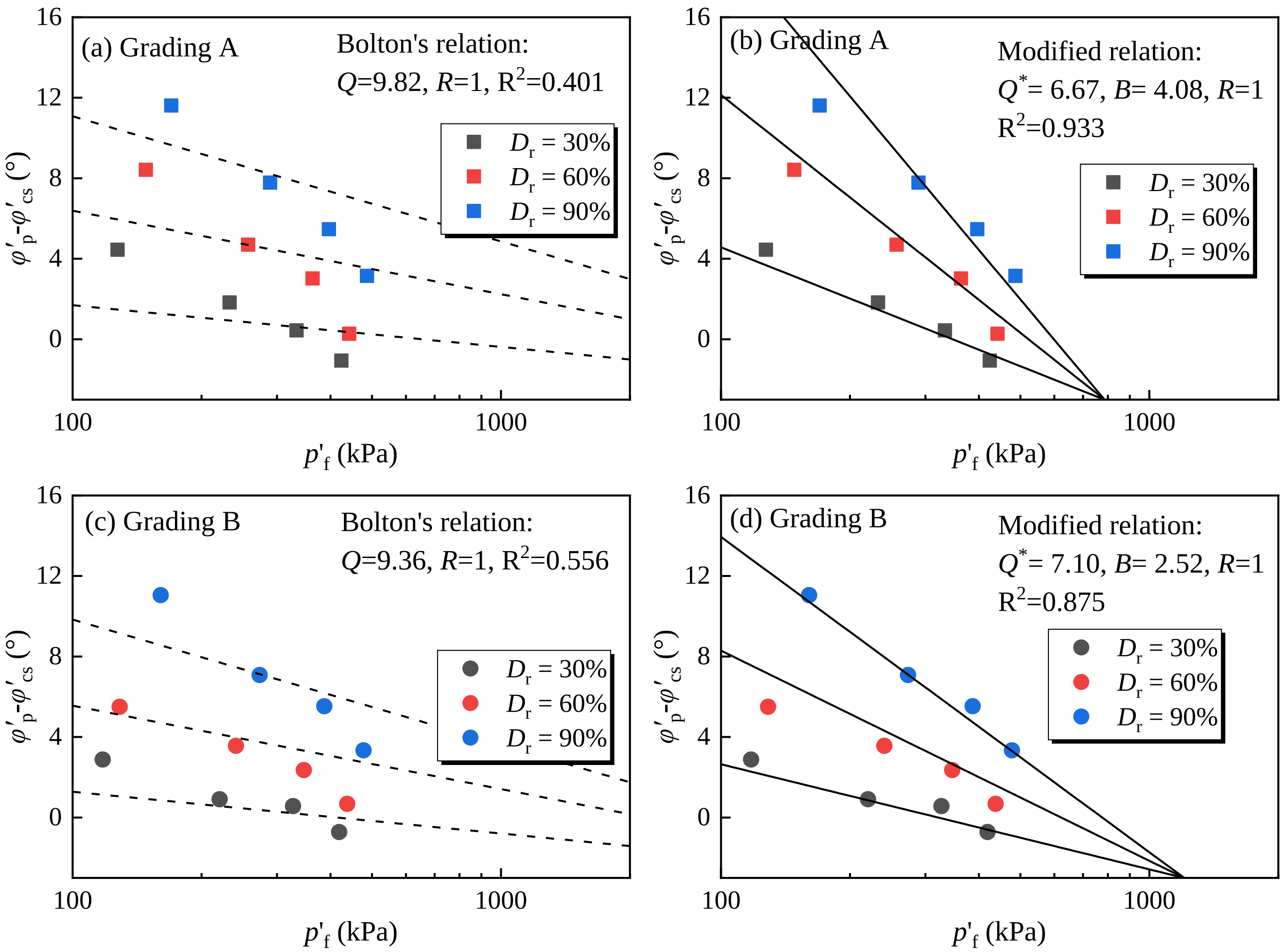

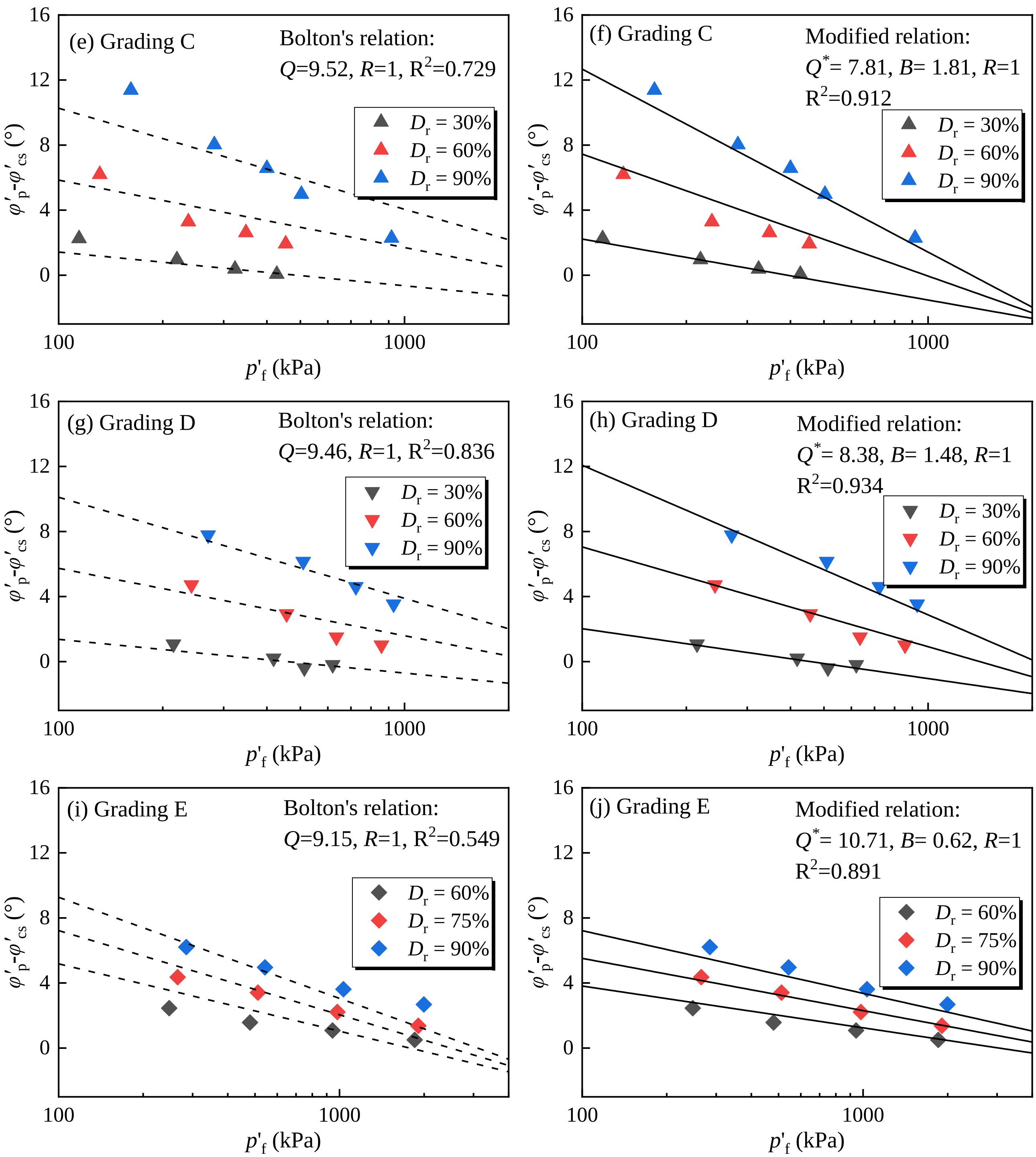

Figure 7 Comparison of the original and modified relation using experimental data of the carbonate soils with (a)-(b) grading A; (c)-(d) grading B; (e)-(f) grading C; (g)-(h) grading D; (i)-(j) grading E

The difference in the fitting results between the two strength-dilatancy relations is significant for very crushable samples (e.g., samples with gradings A and B), but negligible for samples that are difficult to break (e.g., samples with gradings D and E). Carbonate particles regardless of their size, are almost equally angular and elongated as shown in Figure 4 and Table 4. If they are surrounded by grains of a similar size, they will naturally trap a large void fraction. The interlocked grains may fracture when placed in an assembly under deviatoric stress, repacking themselves in a denser arrangement. However, if the larger grains are surrounded by smaller grains, e.g. gradings B to E, the magnitude of intergranular forces acting on the larger grains will be much reduced when the number of contacts increases. The same level of protection against fracture will be provided to each grain size of a distribution, depending on the initial PSD.

It is worth noting that the smallest grain size for gradings A-D samples is 0.5-1 mm, while the grading E samples contain approximately 20% silt fractions, which may lead to a different failure mode, for example, a bulging failure mode was observed for the gradings A-D samples, while a shear band failure mode was observed for the grading E sample. Fine content has been reported to influence the strength and dilatancy behaviour of soils (Salgado et al., 2000; Xiao et al., 2014), which may consequently affect the magnitude of Q^*. Further investigation into the influence of fine content is needed in future studies.

Although Vaid and Sasitharan (1992) suggested that b = 0.33 of Equation (1a) for Erksak sand regardless of triaxial stress path, Bolton's equation suggested that parameter b equals 0.48 for silica sands regardless of the initial PSDs. This means that the difference in friction angle at peak state φ'_p-φ'_{cs} is approximately half of the peak dilatancy angle. Figure 8 shows that b=0.48 fits well within the maximum margin of ±1.5°, the same value as suggested by Bolton (1986). This also supports that the relationship between φ'_p-φ'_{cs} and ψ_{max} is unique regardless of the initial PSD and the crushability of soils.

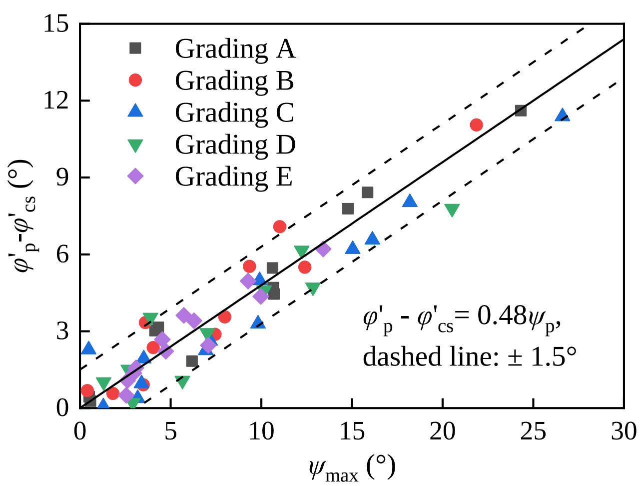

Figure 8 The relationship between the difference in friction angle φ'_p-φ'_{cs} and peak dilatancy angle ψ_{max}

3.4 Correlation of parameters Q^* and B with soil crushability

As aforementioned, Q^* may be related to soil crushability. For a soil sample, its crushability depends on many factors, such as mineralogy, particle size, particle shape, intra-particle structure, and the initial PSD of a soil sample. At present, the authors could not find a comprehensive definition of crushability in the literature, the concept of crushability is primarily qualitative. For example, carbonate soils with weaker grains tend to be more crushable compared to silica soils, and a uniform-graded sample of the same material is more crushable than a well-graded sample. The question then arises how to quantify the crushability of a soil.

As the name implies, crushability should represent the ability of soils to be crushed. This means that, under the same conditions, the greater the degree of particle breakage of a soil, the larger its crushability. To quantify the crushability, we follow a three-step approach:

- Select a suitable breakage index to compute the degree of particle breakage;
- Establish a correlation between the breakage index and the total energy input;
- Obtain a crushability indicator based on the above correlation.

At present, many breakage indices have been proposed to quantify the degree of particle breakage. Although the relative breakage indices B_r (Hardin, 1985) and B_r^* (Einav, 2007) are widely used, the calculations of these indices are based on the initial PSD of a soil, which might make it difficult to compare the degree of particle breakage of soils with different initial PSDs. Khonji et al. (2020) conducted a comparison of five different crushing indices using a large number of breakage data. They found that Marsal's index B_g (Marsal, 1967) provided the best description of the evolution of breakage behaviour. Marsal's breakage index B_g is therefore adopted in this paper. This index is calculated based on the percentage difference in the mass of each size fraction before and after tests, and is independent of the initial PSD. Additionally, the breakage index B_g can also be interpreted as the maximum difference value of the percentage finer between the two PSDs, as shown in Figure 9.

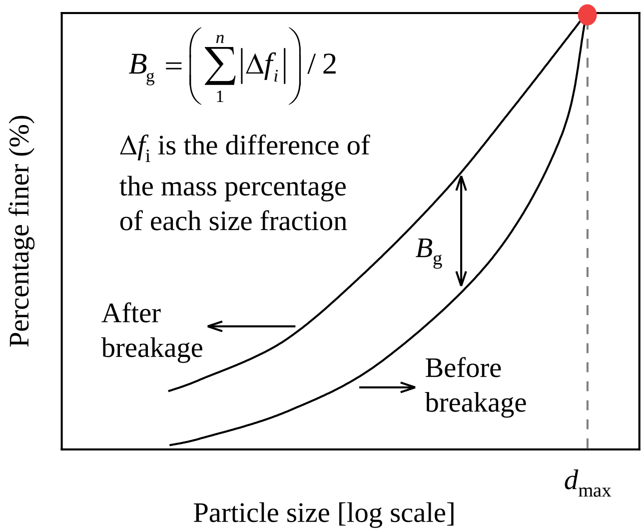

Figure 9 Schematic representation of Marsal's breakage indices B_g (Marsal, 1967)

Many attempts have been made to study the evolution of particle breakage from the perspective of energy input, transformation, and dissipation (McDowell and Bolton, 1998; Tong et al., 2020; Tong et al., 2022a). In this paper, the total energy input during triaxial shearing has been adopted to correlate breakage induced by shearing. The total energy input per volume E_T during the shear stage can be expressed as follows (Lade et al., 1996), where the summation is applied between BOS (beginning of shear) to EOS (end of shear).

$$E_T = \sum_{BOS}^{EOS} (\sigma'_1 - \sigma'_3) \cdot d\varepsilon_1 + \sum_{BOS}^{EOS} \sigma_c \cdot d\varepsilon_v \tag{8}$$

Figure 10 (a) plots the relationship between breakage index B_g and total energy input E_T for the carbonate soils with gradings A-D. It is clear that grading A samples experience the most particle breakage, while grading D samples exhibit the lowest degree of particle breakage for a given E_T. The relationship between B_g and E_T can be expressed as the following hyperbolic function (Lade et al., 1996):

$$B_g = \frac{E_T}{a \times p'_r + E_T} \tag{9}$$

where a is a fitting parameter, p'_r is the reference pressure (= 1000 kPa) for dimensional consistency.

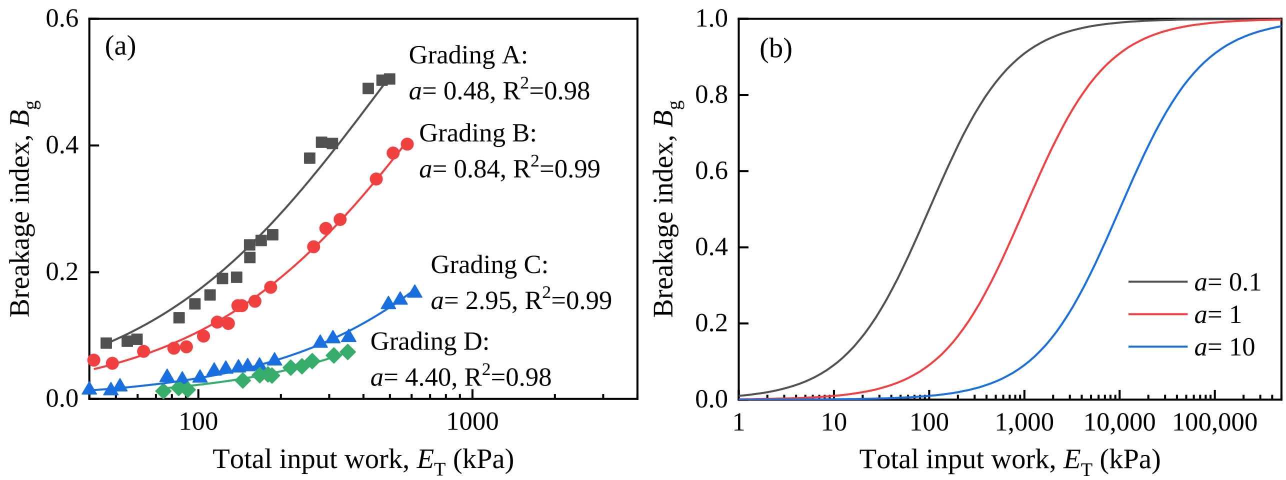

Figure 10 (a) The relationship between breakage index B_g against total energy input per volume E_T of the carbonate soils; (2) B_g-E_T curves with different values of parameter a

As shown in Figure 10(b), the evolution of particle breakage is controlled by parameter a. Soil with a lower a value exhibits early and more pronounced particle breakage. Robustness is defined as the ability of a system to resist change. A lower robustness implies a higher susceptibility of the system to change. Therefore, parameter a serves as a granular robustness indicator, with a smaller value of a indicating higher crushability.

Figure 11 presents the relationship between the parameters Q^*, B and the granular robustness indicator a of the carbonate soils in this paper and other published data on carbonate soils and coarse aggregates from different regions. As the value of parameter a increases, parameter B gradually decreases, approaching 1, and it is observed that its value is larger for coarse aggregates than for carbonate soils. The exact relation between parameter B and the physical properties still needs more comprehensive and in-depth research in the future. However, the parameter Q^* increases with the robustness indicator a for both the carbonate soils and the coarse aggregates. This supports the speculation that the parameter Q^* is related to soil crushability. Parameter B is related to the decreasing rate of φ'_p-φ'_{cs} with $\ln p'_f$ whose physical meaning is encapsulated in the parameter Q^* (=Q/B). For grading E samples in this paper, no detectable particle breakage was observed, indicating an infinite value of the robustness indicator a in Equation (9). Also, Q^* is equal to 10.71 (see Figure 7 (j)). Therefore, we hypothesize that Q^* will approach a value of approximately 10 as crushability decreases. This is consistent with Bolton's equation (Bolton, 1986), where Q is set to 10 for silica sands.

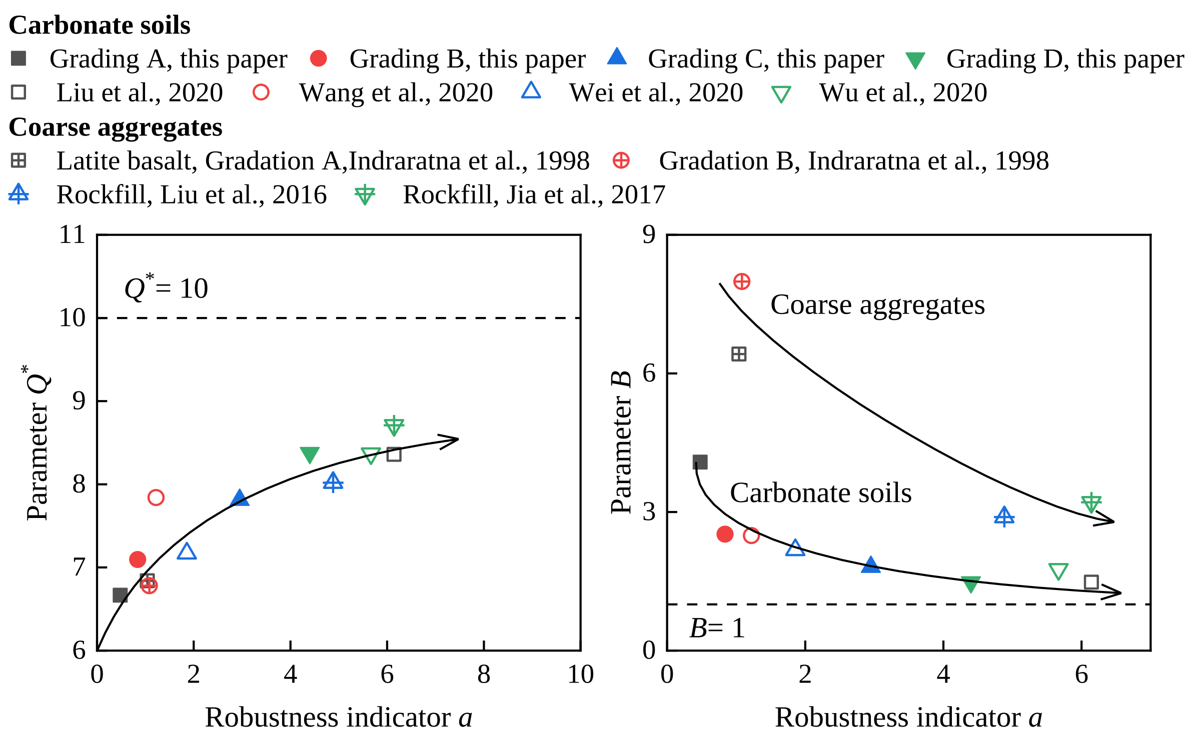

Figure 11 The relationship between parameters Q^* and B with the granular robustness indicator a of crushable soils in this paper and in the literature

4. Model validation using other experimental studies

To validate the modified strength-dilatancy relation, different types of granular soils, such as carbonate soils, coarse aggregates, limestone, anthracite, chalk, and silica sands, as mentioned in Section 2.1 are adopted for analysisand the data are summarized in Table 5. For comparison, Figures 12-15 present the fitting performance of both the original and modified relations. In these figures, the fitting results of the modified relation are depicted using solid lines, while those of the original relation are illustrated with dotted lines.

Table 5 Summary of soil's properties and empirical parameters of the modified relation

Martials		Description	d_{50}	C_u	φ'_{cs}	Q^*	B	Reference
Carbonate soils	Grading A	Highly angular	3.50	1.16	39.89	6.67	4.08	This paper
	Grading B		3.34	4.65	39.16	7.10	2.52	
	Grading C		2.16	3.43	39.01	7.81	1.81	
	Grading D		0.91	1.96	38.17	8.38	1.48	
	Grading E		0.69	29.73	41.08	10.71	0.62	

	Sand A	Angular to subrounded	0.97	1.46	41.70	7.41	2.60	Datta et al., 1979
	Sand D	Subrounded	0.24	1.53	41.70	9.79	1.02	
	—	Highly angular	0.55	2.70	38.19	8.36	1.48	Liu et al.,2020
	—		0.70	1.16	40.71	7.84	2.49	Wang et al., 2020
	—		1.50	1.45	38.99	7.17	2.18	Wei et al., 2021
	—		0.16	1.00	43.44	7.76	1.81	Shen et al., 2021
	—		0.32	2.85	42.00	8.37	1.76	Wu et al., 2021
	Chiibishi sand	Platey to rounded	0.68	2.39	42.58	7.72	1.89	Kuwajima et al., 2009
	Dogs Bay sand		0.22	1.77	42.92	6.53	2.42	
Rockfill	—	Angular sandstone	4.18	—	38.67	7.46	3.43	Charles and Watts, 1980
Rockfill	Gradation A	Sedimentary rock; mainly quartz	4.90	6.00	32.35	7.38	4.37	Indraratna et al., 1993
	Gradation B		3.60	6.00	32.84	7.68	3.35	
Latite basalt	Gradation A	Highly angular	38.90	1.52	45.58	6.84	6.42	Indraratna et al., 1998
	Gradation B		30.30	1.58	45.58	6.78	7.99	
Rockfill	Rockfill A	Rounded andesite	5.87	22.09	46.50	9.06	1.27	AtashBahar et al., 2015
	Rockfill B	Rounded dolomite	5.87	22.09	41.84	7.97	2.33	
	Rockfill C	Rounded dolomite	0.80	3.60	40.63	7.38	3.38	
Rockfill	—	Angular quarried material	15.72	17.25	43.71	8.02	2.89	Liu et al., 2016
Rockfill	—	Granite	19.38	—	38.28	8.48	2.51	Guo and Zhu, 2017
Rockfill	—	Moderately weathered basalt	24.16	6.93	41.22	8.71	3.21	Jia et al., 2017
Gravel	d_{50}=25 mm	Highly angular; dominant mineral: CaO and Fe_2O_3	25.00	1.00	39.50	7.62	2.18	Alhani et al., 2020
	d_{50}=20 mm		20.00	1.00	40.00	7.52	1.92	
	d_{50}=14mm		14.00	1.00	39.39	7.58	1.78	
	d_{50}=10 mm		10.00	1.00	40.25	7.37	1.60	
	d_{50}=5 mm		5.00	1.00	39.58	7.54	1.37	
Open-graded aggregates	d_{50}=17.02 mm	Subrounded grains	17.02	1.72	39.01	6.78	3.41	Nicks and Adams, 2018
	d_{50}=10.67 mm		10.67	2.63	38.92	7.64	2.42	
	d_{50}=8.64 mm		8.64	2.01	39.60	8.49	1.85	
	d_{50}=7.11 mm		7.11	0.79	36.72	8.16	1.74	

	d_{50}=1.27 mm		1.27	9.92	37.83	10.56	1.24	
Limestone	σ_0=3.5 MPa	Angular	—	—	—	5.86	2.56	Lee, 1992
	σ_0=7.0 MPa	Angular	—	—	—	7.18	1.45	
	—	Angular	15.75	1.54	41.39	7.19	2.67	Duncan et al., 2007
	—	Angular	13.88	2.51	41.39	7.43	2.36	Knierim, 2014
	—	—	—	4.29	43.18	8.30	1.32	Billam, 1972
Anthracite	—	—	—	1.64	36.82	7.04	1.14	
Chalk	—	—	—	1.53	46.83	4.62	2.30	
Silica sands	Fulung sand	Subangular	0.20	1.40	33.33	9.85	1.09	Ueng and Chen, 2000
	Toyoura sand	Subrounded	0.65	1.60	31.36	10.92	1.02	Kuwajima et al., 2009
	Toyoura sand	Subrounded	0.20	1.30	33.45	10.23	1.09	Sun et al., 2007
	LBS, σ_0=26 MPa	Rounded	—	—	—	9.68	1.08	Lee, 1992
	LBS, σ_0=26 MPa	Rounded	—	—	—	10.11	1.02	
	Ottawa sand	Rounded	—	—	—	10.90	1.22	Lee and Seed, 1967
	Ottawa sand	Rounded	0.56	1.32	31.80	10.49	1.37	Datta et al., 1979

Note: σ_0 refers to the characteristic stress of single particle crushing (McDowell and Bolton,1998); LBS refers to Leighton Buzzard sand.

4.1 Data of carbonate soils

Figure 12 presents the fitting results for various carbonate soils in the literature to the modified relation, the values of parameters Q^* and B are also shown in the Table 5. The data collected show that Q^* ranges from 6.5 to 9.79, and B ranges from 1.02 to 2.60. In the data from Datta et al. (1979), illustrated in Figures 12(a), both Sand A and Sand D share the same C_u value. However, due to Sand A's the larger mean particle size (d_{50} = 0.97 mm) compared to Sand D (d_{50} = 0.24 mm), Sand A exhibits a smaller Q^* value (= 7.4) in contrast to Sand D's Q^* (= 9.8). Additionally, the value of B decreases from 2.60 for Sand A to 1.02 for Sand D. For other carbonate soils from the South China Seas in Figure 12 (b)-(e), the values of Q^* are similar around 7.2-8.4, and B values are around 1.5-2.5.

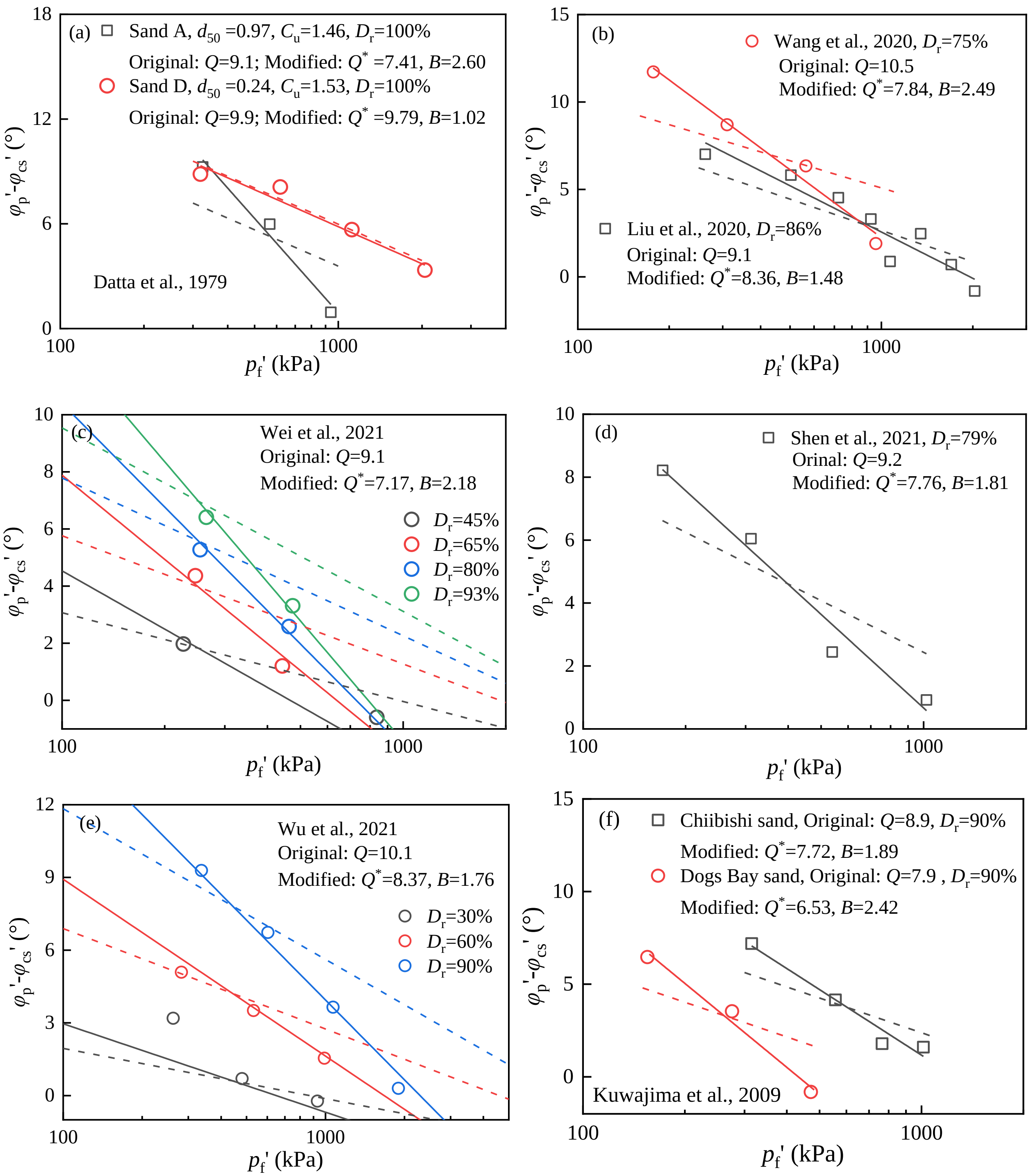

Figure 12 Performance of the original and modified relations using published data of carbonate soils, with solid lines representing the modified relation and dotted lines representing the original relation

4.2 Data of coarse aggregates

Figure 13 presents the fitting results of the modified relation for some coarse aggregates in the literature, with parameter Q^* ranging from 6.78 to 10.56, and parameter B ranging from 1.24 to 7.99. For example, in Figure 13(g), Alhani et al (2020) tested five uniform-graded gravels with d_{50} decreasing sequentially from 25 mm to 5 mm. The value of Q^* increases from 6.78 to 10.56 and B decreases from 2.18 to 1.37. Nicks and Adams (2018) conducted a large amount of drained shearing tests on open-graded aggregates, including four uniform-graded aggregates as shown in Figures 13(h)~(k), and one well-graded aggregate as shown in Figure 13(l). For the aggregates with initial uniform PSDs (C_u <2.63), as the d_{50} decreases sequentially from 17.02 mm to 7.11 mm, Q^* increases from 6.78 to 8.16, while B decreases from 3.41 to 1.24. The well-graded sample (C_u = 9.92) exhibited a Q^* value of 10.56 and a B value of 1.24. The maximum value of Q is 10 for silica sands in Bolton's equation. But for coarse aggregates, the optimal fitting value of Q may exceed 10, as shown in Figure 13 (c). Adopting a maximum Q value of 10 results in a less satisfactory fitting result.

In Equation (3), B was introduced to modify the initial relative density to better control dilatancy, which is related to the slope of φ'_p-φ'_{cs} with lnp'_f, as shown in Figure 3(b). Comparing the data for a given relative density in Figures 13(h) - (l), B is equal to 3.41 for the soil with d_{50} = 17.02 mm (the largest slope), and decreases to 1.24 for the soil with d_{50} = 1.27 mm (the smallest slope). For soils that are more susceptible to crushing, a larger value of B is required to amplify the initial relative density for a better fitting.

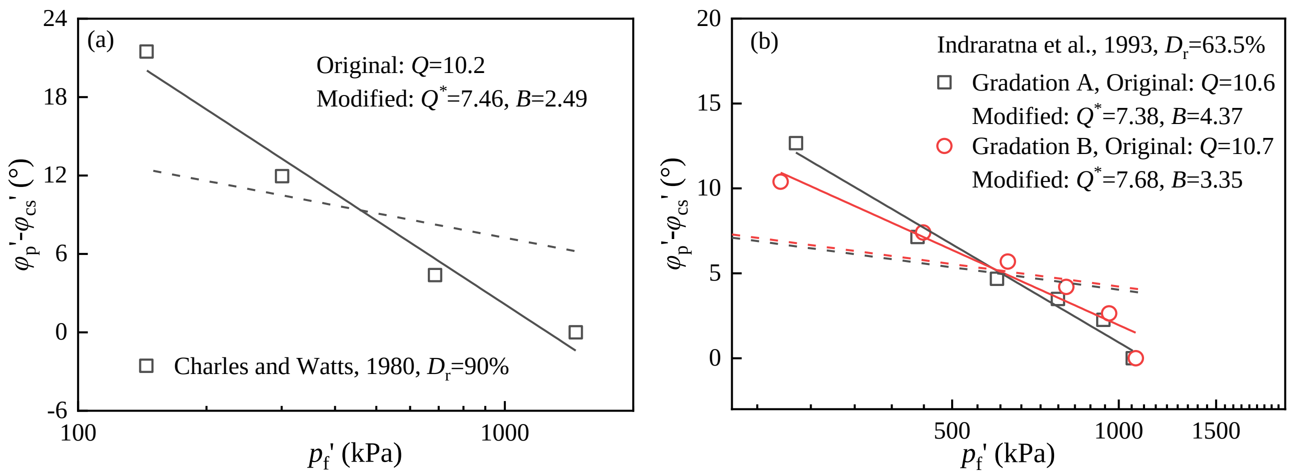

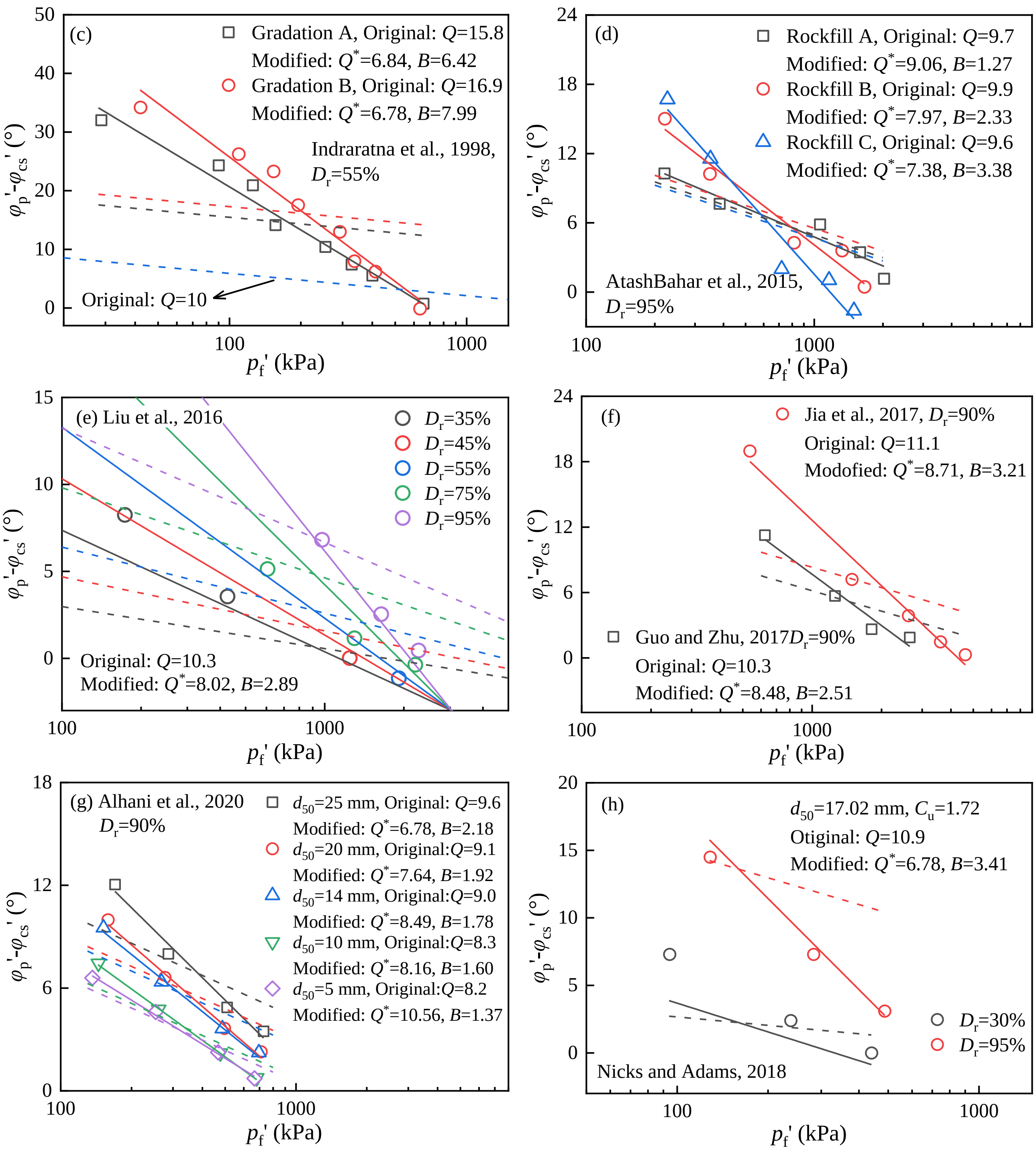

(c)
Gradation A, Original: Q=15.8
Modified: Q*=6.84, B=6.42
Gradation B, Original: Q=16.9
Modified: Q*=6.78, B=7.99
Indraratna et al., 1998,
Dr=55%
Original: Q=10
φp'-φcs' (°)
pf' (kPa)
(d)
Rockfill A, Original: Q=9.7
Modified: Q*=9.06, B=1.27
Rockfill B, Original: Q=9.9
Modified: Q*=7.97, B=2.33
Rockfill C, Original: Q=9.6
Modified: Q*=7.38, B=3.38
AtashBahar et al., 2015,
Dr=95%
(e) Liu et al., 2016
Dr=35%
Dr=45%
Dr=55%
Dr=75%
Dr=95%
Original: Q=10.3
Modified: Q*=8.02, B=2.89
(f)
Jia et al., 2017, Dr=90%
Original: Q=11.1
Modofied: Q*=8.71, B=3.21
Guo and Zhu, 2017Dr=90%
Original: Q=10.3
Modified: Q*=8.48, B=2.51
(g) Alhani et al., 2020
Dr=90%
d50=25 mm, Original: Q=9.6
Modified: Q*=6.78, B=2.18
d50=20 mm, Original:Q=9.1
Modified: Q*=7.64, B=1.92
d50=14 mm, Original:Q=9.0
Modified: Q*=8.49, B=1.78
d50=10 mm, Original:Q=8.3
Modified: Q*=8.16, B=1.60
d50=5 mm, Original:Q=8.2
Modified: Q*=10.56, B=1.37
(h)
d50=17.02 mm, Cu=1.72
Otiginal: Q=10.9
Modified: Q*=6.78, B=3.41
Dr=30%
Dr=95%
Nicks and Adams, 2018

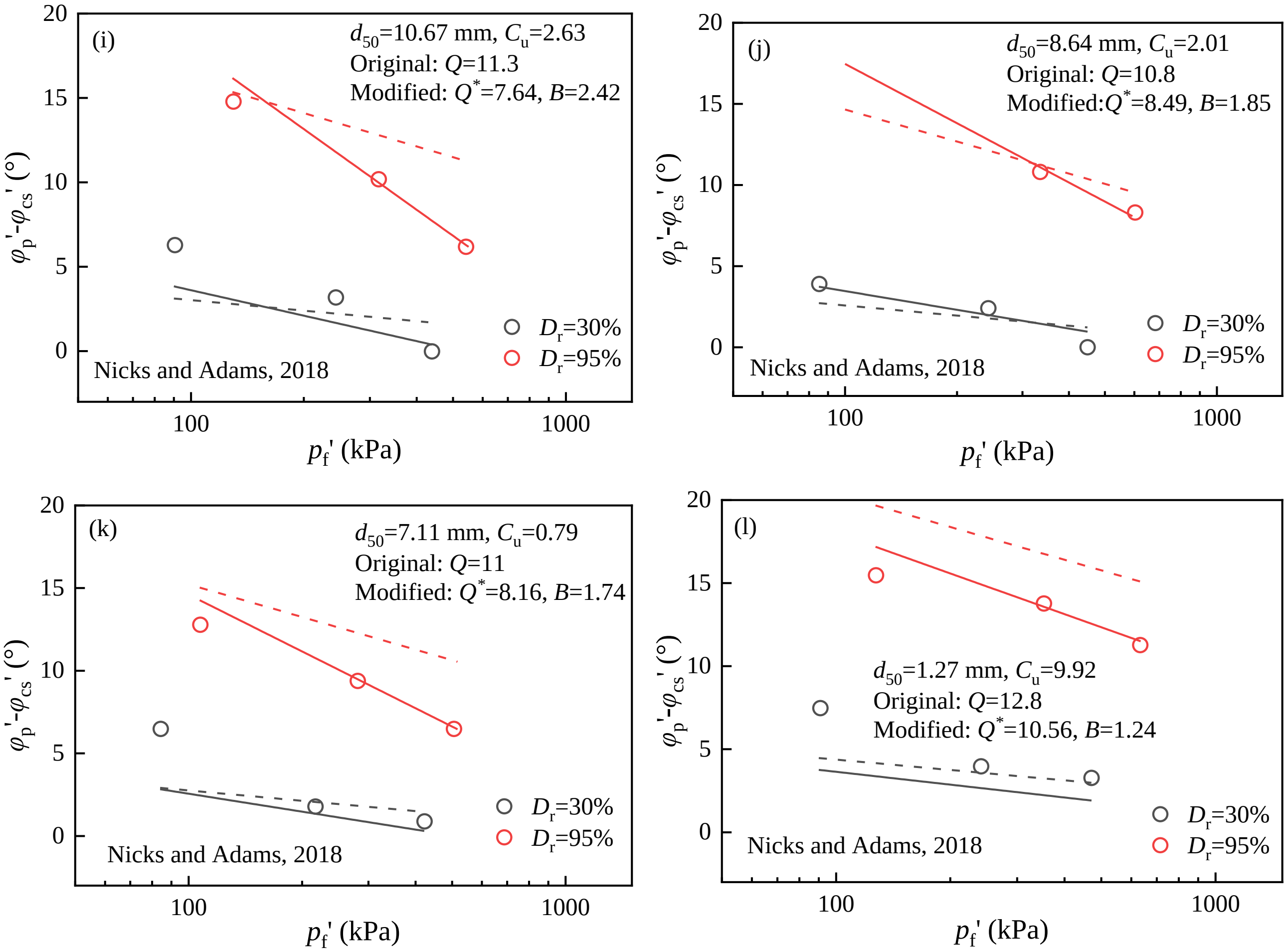

Figure 13 Performance of the original and modified relations using published coarse aggregates data, with solid lines representing the modified relation and dotted lines representing the original relation

4.3 Data of materials used in Bolton's paper

Bolton suggested smaller Q for soils with weaker grains using data from Billam (1972). Specifically, Q values of 8 were recommended for limestone, 7 for anthracite, and 5.5 for chalk. These crushable materials were also fitted using the modified relation, as shown in Figures 14(a) - (c). It can be seen that the performance of the modified relation is better, especially for the fragile granulated chalk. Comparing the range of published limestone data shown in Figures 14(a), (d), (e), and (f), the best-fit values of Q^* and B are different. This indicates that using a fixed value of Q (e.g., Q= 8 for limestone as suggested by Bolton (1986)) is not appropriate. Although Q was believed to be related to crushability, crushability could be affected by many factors including particle size, particle shape, inter-particle defects, and initial PSD. A relatively wide range of values for both Q^* and B is observed for a material, which is consistent with the triaxial test data of the carbonate soils presented earlier in this paper.

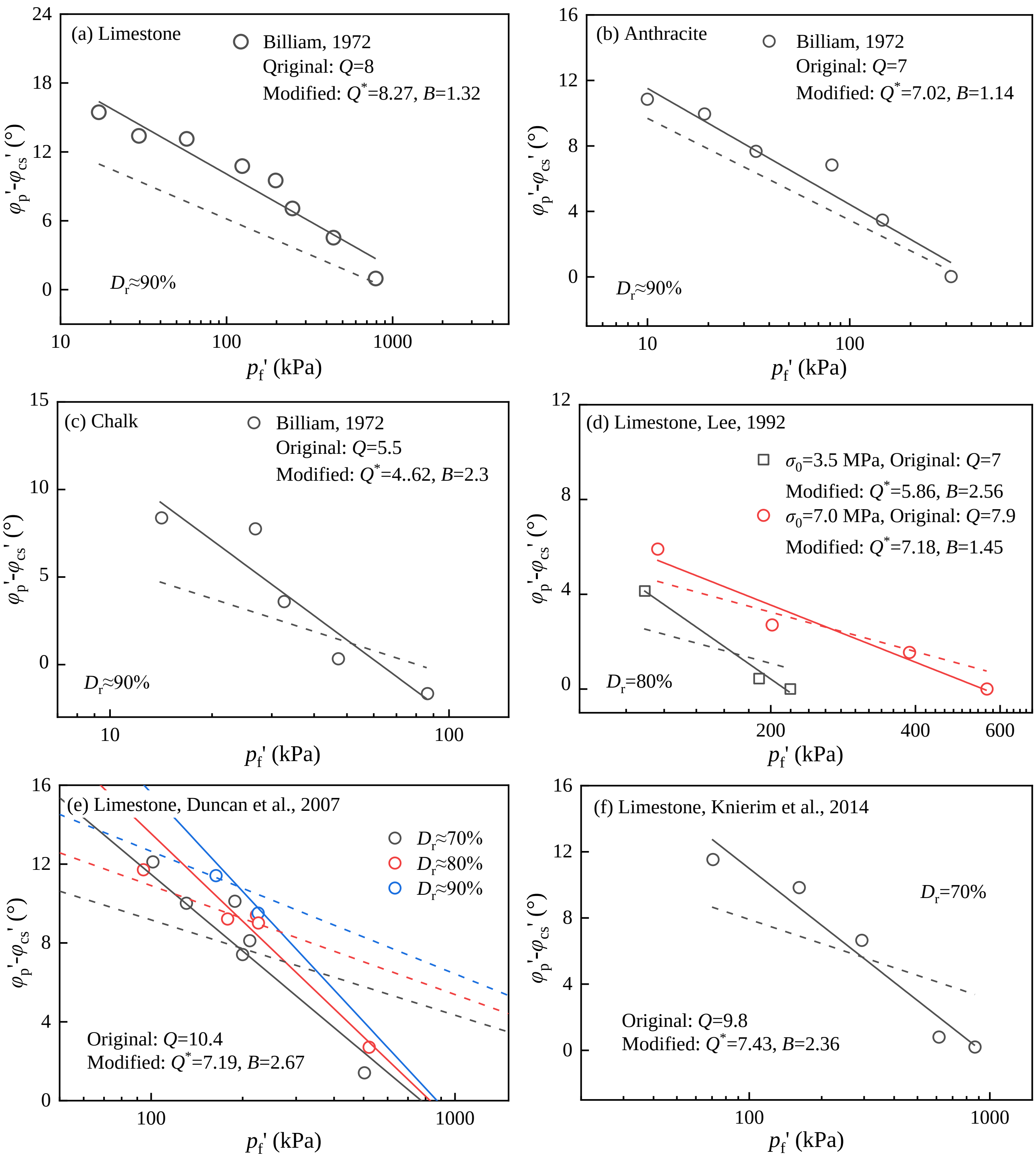

Figure 14 Performance of the original and modifieds relation using published data of limestone, anthracite and chalk, with solid lines representing the modified relation and dotted lines representing the original relation

4.4 Data of silica sands with particle breakage observed

Although Bolton's equation considers the effect of particle breakage, the validation is mainly focused on silica sands. Compared to carbonate soils, coarse aggregates, limestone, anthracite, and chalk, silica particles exhibit greater strength and a more subrounded to rounded shape. Consequently, they experience lower levels of particle breakage, while surface grinding and asperity breakage may occur during shearing. Published drained triaxial data for silica sands was collected and fitted using the original and modified relation (Ueng and Chen, 2000; Kuwajima et al., 2009; Sun et al., 2007; Lee, 1992; Lee and Seed, 1967; Datta et al., 1979). The fitting results are shown in Figure 15 with Q = 10 for silica sands as suggested by Bolton (1986). It can be seen that Bolton's equation performs better for less crushable silica sands. For the fitting of the modified relation, the value of parameter Q^* fluctuates around 10 and parameter B fluctuates around 1, indicating that the modified relation yields to Bolton's original equation.

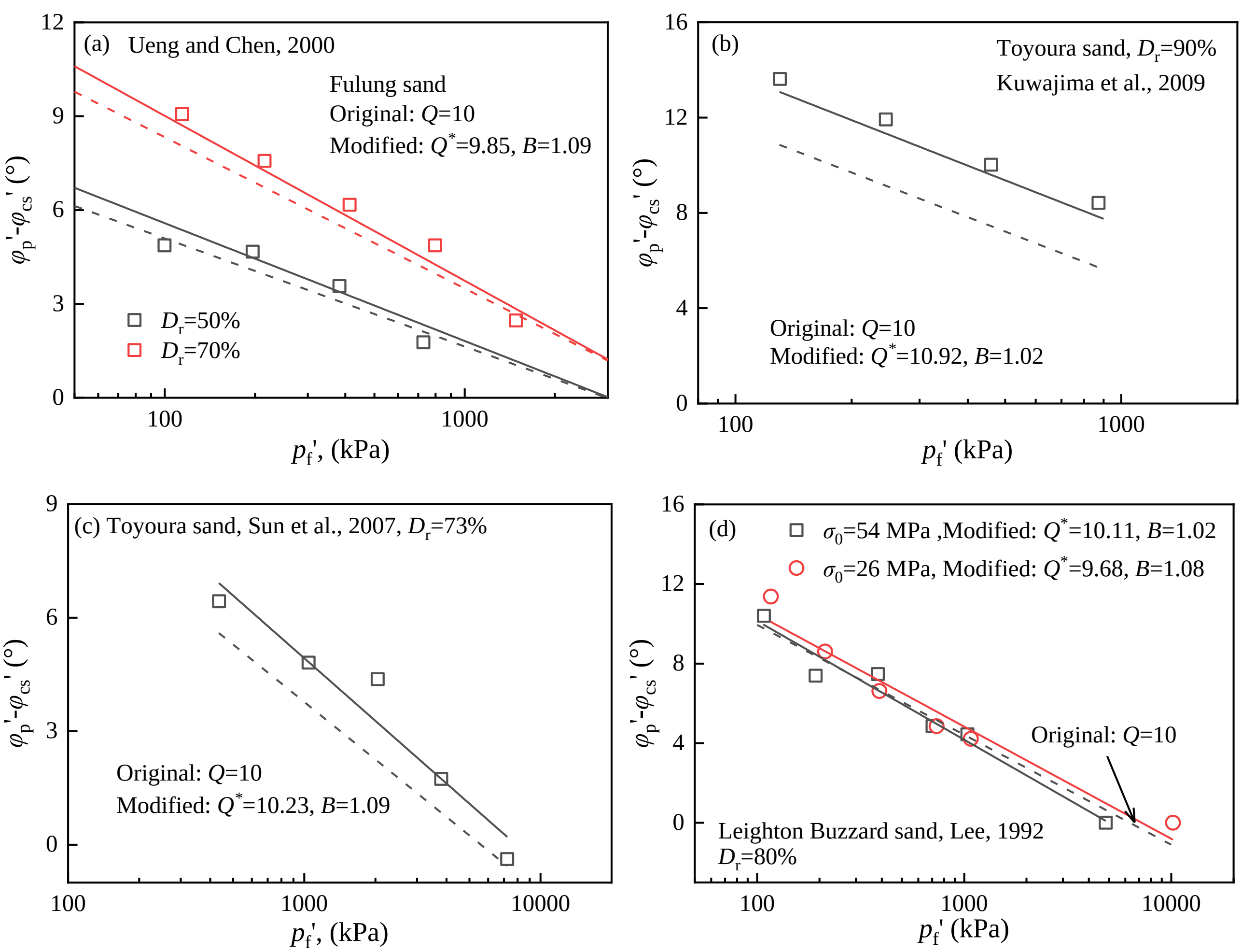

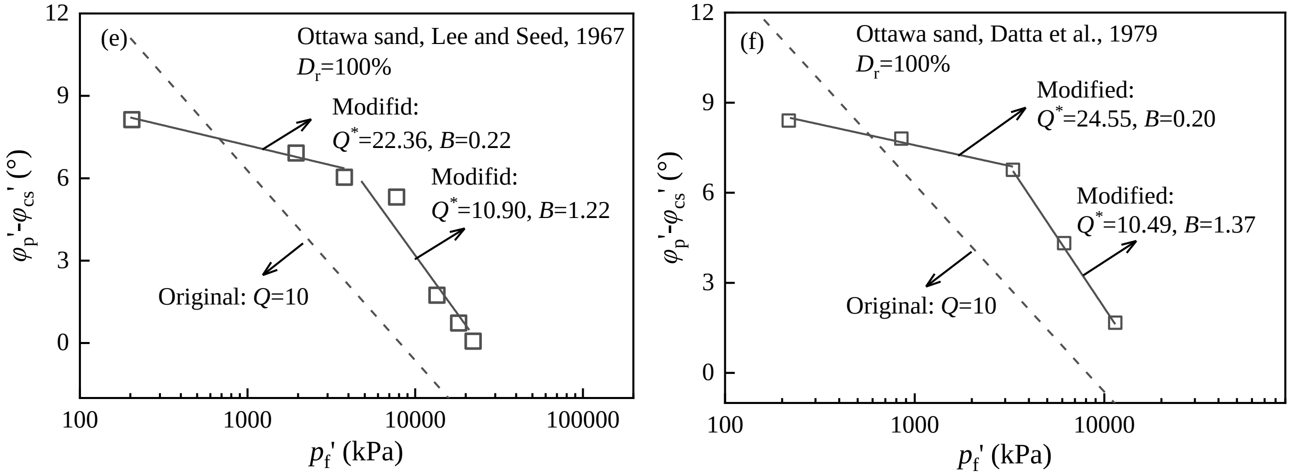

Figure 15 Performance of the original and modified relations using published data of silica soils, with solid lines representing the modified relation and dotted lines representing the original relation

For the Ottawa sand data, as shown in Figures 15(e) and (f), there are two distinct slopes for p'_f smaller than and larger than around 3 MPa. Q^* is around 10 and B is around 1 when p'_f is larger than 3 MPa. However, Q^* is significantly large up to 24.55 for p'_f values below this threshold. Bolton (1986) also found that some initially rounded silica sands experienced minimal changes in their friction angle, and the original equation is only applicable when the stress exceeds a certain threshold. In this case, the threshold stress for Ottawa sand is approximately 3 MPa. When fitted against the modified equation in this region, Q^* is significantly larger than 10, and B is relatively small. They are out of the range of most datasets, and further investigation is required.

5. Conclusions

Bolton's strength-dilatancy relation (Bolton, 1986) is modified by introducing one empirical parameter B. The modified relation is then validated against a series of drained triaxial tests on carbonate soils as well as against experimental data from the literature. The following conclusions are drawn from the study:

1. The modified relation better captures the different decresing rate of φ'_p-φ'_{cs} with effective mean stress at failure lnp'_f for a wider range of crushable soils and gradings than Bolton's equation. This is based on the data of five different particle size distributions of the same carbonate soil, and the data of other crushable soils such as various carbonate soils, coarse aggregates and less crushable silica sands from different regions of the world, as well as the data of limestone sand, crushed anthracite and granulated chalk used by Bolton (1986). The relation between the difference in effective friction angle φ'_p-φ'_{cs}

and the maximum dilatancy angle ψ_p is unique regardless of initial PSD and crushability of soil samples, with b = 0.48 being the same as that suggested by Bolton (1986).

2. The modified relation maintains the simple form of Bolton's strength-dilatancy equation without changing the values of the original fitting parameters in Equation (1): b = 0.48, m = 3, R =1 for triaxial condition. Both the original and modified relations represent sets of straight lines converging at a point in $(\varphi'_p-\varphi'_{cs})$-ln$p'_f$ plane. The convergent stress p_c, whose natural logarithm is equal to Q^*, is independent of the initial relative density and stress. The parameter Q^* tends to decrease with increasing soil crushability. The parameter B is related to the slope of $\varphi'_p-\varphi'_{cs}$ with lnp'_f. For materials that are more susceptible to crushing, a larger B is required to modify the initial relative density to better fit data with a larger slope. The variability of Q^* and B for crushable soils with varying mineralogy and initial PSDs strongly suggests that engineers should perform at least two project-specific triaxial tests at appropriate relative densities and effective stresses if the performance of these materials is to be accurately predicted.
3. A correlation was established between the degree of particle breakage and the total energy input during shearing. It is found that the fitting parameter a (Lade et al., 1996) can be used as a granular robustness indicator with a smaller value of a indicating a larger crushability. Soil crushability affects both the parameter Q^* and B in the modified relation. For less crushable materials such as silica sands, Q^* approaches 10 and B approaches 1, indicating that the proposed modified strength and dilatancy relation yields to Bolton's equation.

Acknowledgements

This research was supported by the National Natural Science Foundation of China (Grant No. 52378382, No. 52008402), Natural Science Foundation of Hunan Province (Grant No. 2021JJ40758), The Science and Technology Innovation Program of Hunan Province (2023RC1017), and Innovation-Driven Project of Central South University (Grant No. 2022ZZTS0151). The first author is grateful for the support of the China Scholarship Council for the visit to University College London. The authors would like to thank Professor Malcolm Bolton's for his valuable comments, which significantly improved the overall quality of this paper.

List of symbols:

a granular robustness indicator

b, m, Q, R Q^*, B	parameters of the original and modified relation
B_g	breakage index proposed by Marsal (1967)
B_r, B_r^*	the relative breakage indices proposed by Hardin (1985) and Einav (2007)
C_u, C_c	uniformity coefficient and coefficient of curvature
d	particle size
d_{50}	mean particle size
d_{max}	the maximum particle size
D	fractal dimension
D_r	relative density
e_{max}, e_{min}	the maximum and minimum void ratio
E_b	accumulated particle breakage energy
E_T	the total energy input per volume
G_s	specific gravity
I_R, I^*_R	the original and modified relative dilatancy index
M ($\Delta<d$)	mass of particles with diameter smaller than d
M	friction coefficient used to calculate frictional energy
M_c	critical state stress ratio
M_T	total mass of particles
p'_{crit}	critical mean effective stress in relation to zero dilation
p'_f	mean effective stress at failure
p_r, p'_r	reference pressures, p_r = 1 kPa and p'_r = 1000 kPa
p_c	convergent stress of the original and modified relation
$d\varepsilon_v$, $d\gamma$, $d\varepsilon_1$	volumetric, shear and axial strain increment
σ'_1, σ'_3	the major and minor effective principal stress
φ'_p, φ'_{cs}	effective friction angle at peak and critical state
φ'_u	pure friction angle between the mineral surfaces of grains
ψ_{max}, ψ_p	the maximum dilatancy angle and peak dilatancy angle

Reference

Airey, D. W., Randolph, M. F. & Hyden, A. M. (1988). The strength and stiffness of two calcareous sands. *Proc. Int. Conf. on Engng for Calcareous Sediments, Perth*, Vol. 1, pp. 43–50.

Alhani, I. J., Noor, M. J. B. M., Al-Bared, M. A. M., Harahap, I. S. H., & Albadri, W. M. (2020). Mechanical response of saturated and unsaturated gravels of different sizes in drained triaxial testing. *Acta Geotech*., 15, 3075–3093.

Altuhafi, F. N., Coop, M. R., & Georgiannou, V. N. (2016). Effect of particle shape on the mechanical behavior of natural sands. *J. Geotech. Geoenviron. Eng.*, 142(12), 04016071.

Amirpour Harehdasht, S., Karray, M., Hussien, M. N., & Chekired, M. (2017). Influence of particle size and gradation on the stress-dilatancy behavior of granular materials during drained triaxial compression. *Int. J. Geomech*, 17(9), 04017077.

Amirpour Harehdasht, S., Hussien, M. N., Karray, M., Roubtsova, V., & Chekired, M. (2019). Influence of particle size and gradation on shear strength–dilation relation of granular materials. *Can. Geotech. J*, 56(2), 208–227.

Arda, C., & Cinicioglu, O. (2021). Influence of grain shape on stress-dilatancy parameters. *Granul. Matter*, 23, 1–19.

ASTM (2020) Standard test method for consolidated undrained triaxial compression test for cohesive soils. ASTM D4767-11West Conshohocken, PA: ASTM International.

ASTM (2014). Standard test method for sieve analysis of fine and coarse aggregates. ASTM C136/ C136M-14, West Conshohocken, PA: ASTM International.

AtashBahar, M., Chenari, R. J., & Neshaei, M. A. L. e. (2015). Evaluation of the behavior of rockfill material using large-scale triaxial tests. *Proc. 2nd Int. Conf. Geotech. Urban Earthq. Eng.*, Tabriz.

Baldi, G., & Nova, R. (1984). Membrane penetration effects in triaxial testing. *J. Geotech. Engrg.*, 110(3), 403–420.

Been, K., & Jefferies, M. G. (1985). A state parameter for sands. *Géotechnique*, 35(2), 99–112.

Billam, J. (1972). Some aspects of the behaviour of granular materials at high pressures. Stress-Strain Behaviour of Soils. *Proc. Roscoe Memorial Symp.*, pp, 69–80.

Bolton, M. D. (1986). The strength and dilatancy of sands. *Géotechnique*, 36(1), 65–78.

Chakraborty, T., & Salgado, R. (2010). Dilatancy and shear strength of sand at low confining pressures. *J. Geotech. Geoenviron. Eng*, 136(3), 527–532.

Charles, J. A., & Watts, K. S. (1980). The influence of confining pressure on the shear strength of compacted rockfill. *Géotechnique*, 30(4), 353–367.

Cheng, Y. P., Bolton, M. D., & Nakata, Y. (2004). Crushing and plastic deformation of soils simulated using DEM. *Géotechnique*, 54(2), 131–141.

Cheng, Y. P., Nakata, Y., & Bolton, M. D. (2003). Discrete element simulation of crushable soil. *Géotechnique*, 53(7), 633–641.

China MOHURD. 2019. Standard for geotechnical testing method. GB/T 50123-2019. Ministry of Housing and Urban-Rural Development of the People's Republic of China, Beijing, China.

Coop, M. R., Sorensen, K. K., Bodas Freitas, T., & Georgoutsos, G. (2004). Particle breakage during shearing of a carbonate sand. *Géotechnique*, 54(3), 157–163.

Datta, M., Gulhati, S. K. & Rao, G. V. (1979). Crushing of carbonate sands during shear. *Proc. Offshore Tech. Conf.*

Duncan, J. M. (2007). Densities and friction angles of granular materials with standard gradations 21b and # 57. Center for Geotechnical Practice and Research, The Charles E. Via, Jr. Department of Civil Engineering, Virginia Polytechnic Institute and State University.

Dong, Z. L., Tong, C. X., Zhang, S., Teng, J. D., & Sheng, D. C. (2024) A comparative study on shear behaviour of uniform-, gap- and fractal-gradedcarbonate sands. *J. Geotech. Geoenviron. Eng.*, 150(1), 04023128.

Einav, I. (2007). Breakage mechanics—part I: theory. *J. Mech. Phys. Solids.*, 55(6), 1274–1297.

Fan, K., Zheng, Y., Baudet, B. A., & Cheng, Y. P. H. (2021). Investigation of the ultimate particle size distribution of a carbonate sand. *Soils Found*, 61(6), 1708–1717.

Guo, W. L., & Chen, G. (2022). Particle breakage and gradation evolution of rockfill materials during triaxial shearing based on the breakage energy. *Acta Geotechnica*, 17(11), 5351–5358.

Guo, W. L., & Zhu, J. G. (2017). Particle breakage energy and stress dilatancy in drained shear of rockfills. *Géotechnique Lett.*, 7(4), 304–308.

Hamidi, A., Alizadeh, M., & Soleymani, S. M. (2009). Effect of particle crushing on shear strength and dilation characteristics of sand-gravel mixtures., *Int. J. Civ. Eng.*, 7(1), 61–71.

Hardin, B. O. (1985). Crushing of soil particles. *J. Geotech. Engrg.*, 111(10), 1177–1192.

Indraratna, B., Ionescu, D., & Christie, H. D. (1998). Shear behavior of railway ballast based on large-scale triaxial tests. *J. Geotech. Geoenviron. Eng.*, 124(5), 439–449.

Indraratna, B., Wijewardena, L. S. S., & Balasubramaniam, A. S. (1993). Large-scale triaxial testing of grey wacke rockfill. *Géotechnique*, 43(1), 37–51.

Jamiolkowski, M. B., Lo Presti, D. F. C. & Manassero, M. (2003). Evaluation of relative density and shear strength of sands from cone penetration test. *Soil behaviour and soft ground construction*, ASCE Geotechnical Special Publication 119, pp. 201–238.

Jia, Y., Xu, B., Chi, S., Xiang, B., & Zhou, Y. (2017). Research on the particle breakage of rockfill materials during triaxial tests. *Int. J. Geomech*, 17(10), 04017085.

Khonji, A., Bagherzadeh-Khalkhali, A., & Aghaei-Araei, A. (2020). Experimental investigation of rockfill particle breakage under large-scale triaxial tests using five different breakage factors. *Powder Technol*. 363, 473–487.

Knierim, C. D. (2014). Geotechnical characterization and drained shear strength of a limestone aggregate. MD thesis, Oregon State University.

Kuwajima, K., Hyodo, M., & Hyde, A. F. (2009). Pile bearing capability factors and soil crushabiity. *J. Geotech. Geoenviron. Eng*, 135(7), 901–913.

Lau, C. K., & Bolton, M. D. (2011a). The bearing capacity of footings on granular soils. I: Numerical analysis. *Géotechnique*, 61(8), 627-638.

Lau, C. K., & Bolton, M. D. (2011b). The bearing capacity of footings on granular soils. II: Experimental evidence. *Géotechnique*, 61(8), 639-650.

Lade, P. V., Yamamuro, J. A., & Bopp, P. A. (1996). Significance of particle crushing in granular materials. *J. Geotech. Engrg.*, 122(4), 309–316.

Lee, D. M. (1992). The angles of friction of granular fills. Ph. D thesis, University of Cambridge.

Lee, K. L. & Seed, H. B. (1967). Drained strength characteristics of sands. *J. Soil Mech. Fdns. Div. Am. Soc. Civ. Engrs.*, 93(6), 117-141.

Liu, H., Zeng, K., & Zou, Y. (2020). Particle breakage of calcareous sand and its correlation with input energy. *Int. J. Geomech*, 20(2), 04019151.

Liu, J., Zou, D., Kong, X., & Liu, H. (2016). Stress-dilatancy of Zipingpu gravel in triaxial compression tests. *Sci. China Tech. Sci.*, 59, 214–224.

Marsal, R. J. (1967). Large-scale testing of rockfills materials. *J. Soil Mech. Found. Engng Div. ASCE*, 93(2), 27–44.

McDowell, G. R., & Bolton, M. D. (1998). On the micromechanics of crushable aggregates. *Géotechnique*, 48(5), 667–679.

Nicks, J., & Adams, M. (2018). Impact of initial density on strength-deformation characteristics of open-graded aggregates. FHWA Publication No. FHWA-HRT-18-048, pp, 1–16.

Perkins, S. W., & Madson, C. R. (2000). Bearing capacity of shallow foundations on sand: A relative density approach. *J. Geotech. Geoenviron. Eng.*, 126(6), 521–530.

Phuong, N. T. V., Rohe, A., Brinkgreve, R. B. J., & Van Tol, A. F. (2018). Hypoplastic model for crushable sand. *Soils Found*, 58(3), 615–626.

Rowe, P. W. (1962). The stress–dilatancy relation for static equilibrium of an assembly of particles in contact. *Proceedings of the Royal Society of London. Series A. Mathematical and Physical Sciences*, 269(1339), 500–527.

Salgado, R., Bandini, P. & Karim, A. (2000). Shear strength and stiffness of silty sand. *J. Geotech. Geoenviron. Engng*, 126(5), 451–462.

Salim, W., & Indraratna, B. (2004). A new elastoplastic constitutive model for coarse granular aggregates incorporating particle breakage. *Can. Geotech. J.*, 41(4), 657–671.

Shen, J., Wang, X., Wang, X., Yao, T., Wei, H., & Zhu, C. (2021). Effect and mechanism of fines content on the shear strength of calcareous sand. *B. Eng. Geol. Environ.*, 80, 7899–7919.

Simoni, A., & Houlsby, G. T. (2006). The direct shear strength and dilatancy of sand-gravel mixtures. *Geotech. Geol. Eng*, 24, 523–549.

Sun, D. A., Huang, W. X., Sheng, D. C., & Yamamoto, H. (2007). An elastoplastic model for granular materials exhibiting particle crushing. *Key Eng. Mater.*, 340, 1273–1278.

Tarantino, A., & Hyde, A. F. (2005). An experimental investigation of work dissipation in crushable materials. *Géotechnique*, 55(8), 575–584.

Tong, C. X., Burton, G. J., Zhang, S., & Sheng, D. (2020). Particle breakage of uniformly graded carbonate sands in dry/wet condition subjected to compression/shear tests. *Acta Geotech*., 15, 2379–2394.

Tong, C. X., Zhai, M. Y., Li, H. C., Zhang, S., & Sheng, D. (2022a). Particle breakage of granular soils: changing critical state line and constitutive modelling. *Acta Geotech*., 17, 755–768.

Tong, C. X., Dong, Z. L., Sun, Q., Zhang, S., Zheng, J. X., & Sheng, D. (2022b). On compression behavior and particle breakage of carbonate silty sands. *Eng. Geol*, 297, 106492.

Tyler, S. W. & Wheatcraft, S. W. (1992). Fractal scaling of soil particle size distributions: analysis and limitations. *Soil Sci. Soc. Am. J*, 56(2), 362–369.

Ueng, T. S., & Chen, T. J. (2000). Energy aspects of particle breakage in drained shear of sands. *Géotechnique*, 50(1), 65–72.

Vaid, Y. P., & Sasitharan, S. (1992). The strength and dilatancy of sand. *Can. Geotech. J.*, 29(3), 522–526.

Wan, R. & Guo, P. (1998). A simple constitutive model for granular soils: modified stress–dilatancy approach. *Comput. Geotech.*, 22(2), 109–133.

Wang, G., Wang, Z., Ye, Q., & Wei, X. (2020). Particle breakage and deformation behavior of carbonate sand under drained and undrained triaxial compression. *Int. J. Geomech*, 20(3), 04020012.

Wei, H., Li, X., Zhang, S., Zhao, T., Yin, M., & Meng, Q. (2021). Influence of particle breakage on drained shear strength of calcareous sands. *Int. J. Geomech*, 21(7), 04021118.

Wu, Y., Cui, J., Huang, J., Zhang, W., Yoshimoto, N., & Wen, L. (2021). Correlation of critical state strength properties with particle shape and surface fractal dimension of clinker ash. *Int. J. Geomech*, 21(6), 04021071.

Wu, Y., Li, N., Wang, X., Cui, J., Chen, Y., Wu, Y., & Yamamoto, H. (2021). Experimental investigation on mechanical behavior and particle crushing of calcareous sand retrieved from South China Sea. *Eng. Geol*, 280, 105932.

Xiao, Y., Liu, H., Chen, Y., & Chu, J. (2014). Strength and dilatancy of silty sand. *J. Geotech. Geoenviron. Eng.*, 140(7), 06014007.

Yasufuku, N., & Hyde, A. F. L. (1995). Pile end-bearing capacity in crushable sands. *Géotechnique*, 45(4), 663–676.

Yang, J., & Luo, X. D. (2015). Exploring the relationship between critical state and particle shape for granular materials. *J. Mech. Phys. Solids.*, 84, 196–213.

Zhang J. M. (2000) Study of the fundamental mechanical characteristic of calcareous sand and the influence of particle breakage. Ph. D thesis, Chinese Academy of Science. (in Chinese)

Zhang, X., & Baudet, B. A. (2013). Particle breakage in gap-graded soil. *Géotechnique Lett*, 3(2), 72–77.